Gravitational waves and compact binaries

GGI, Lecture # 5

Enrico Barausse

Institut d’astrophysique de Paris/CNRS, France

H2020-MSCA-RISE-2015 StronGrHEP-690904

This lecture

What is the structure of (isolated or binary) BHs in GR and beyond?

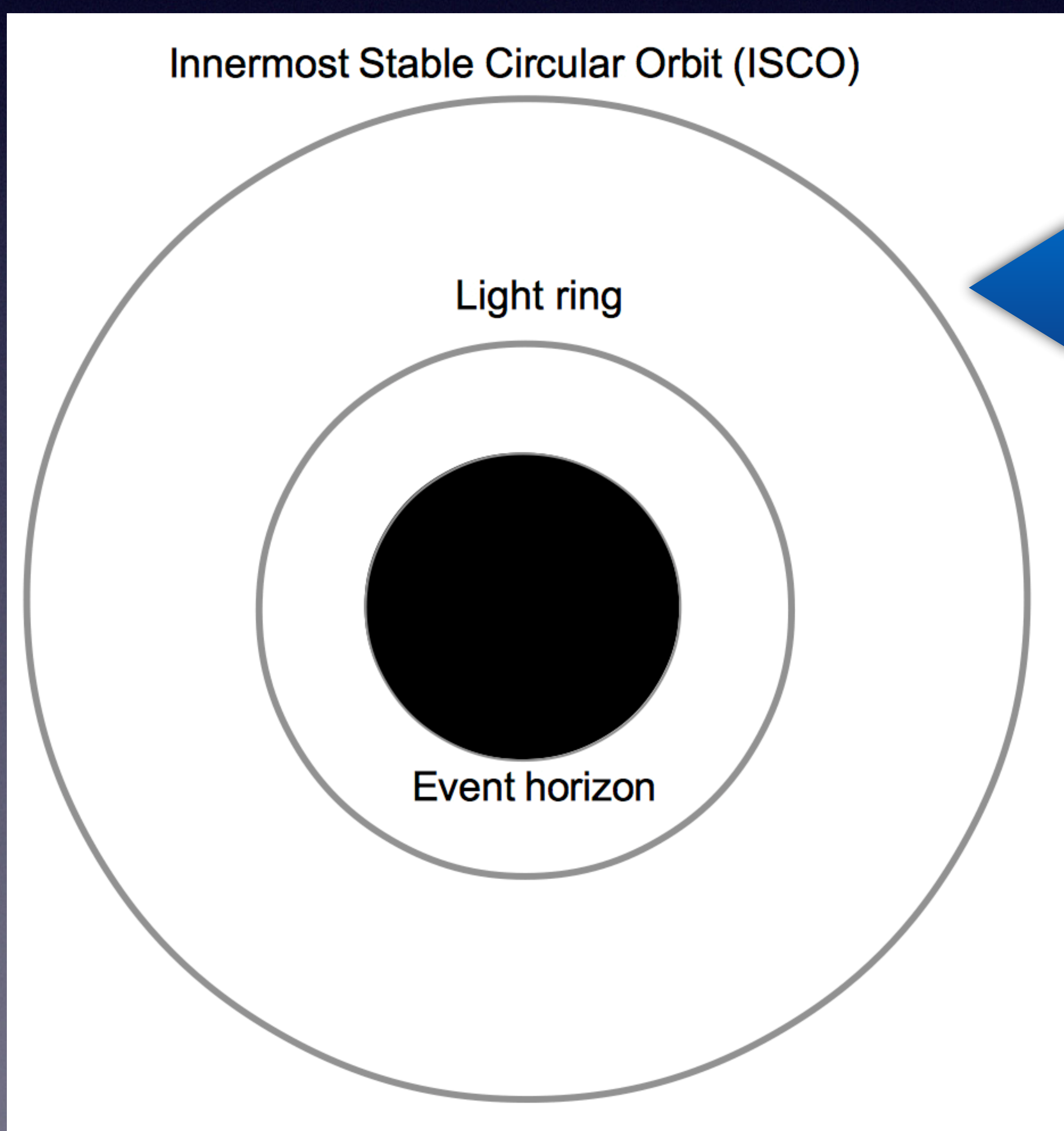

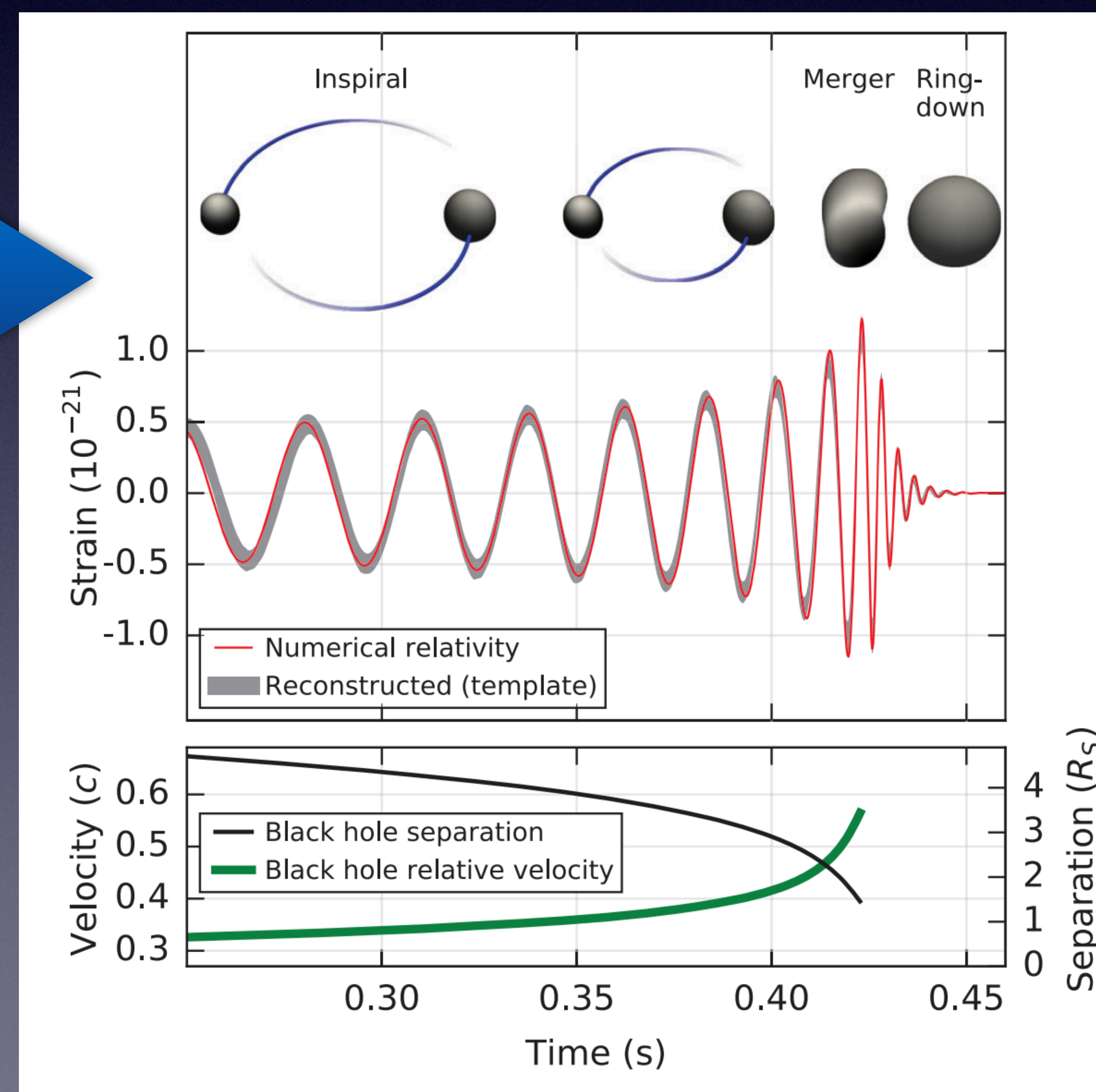

GWs from binary BHs

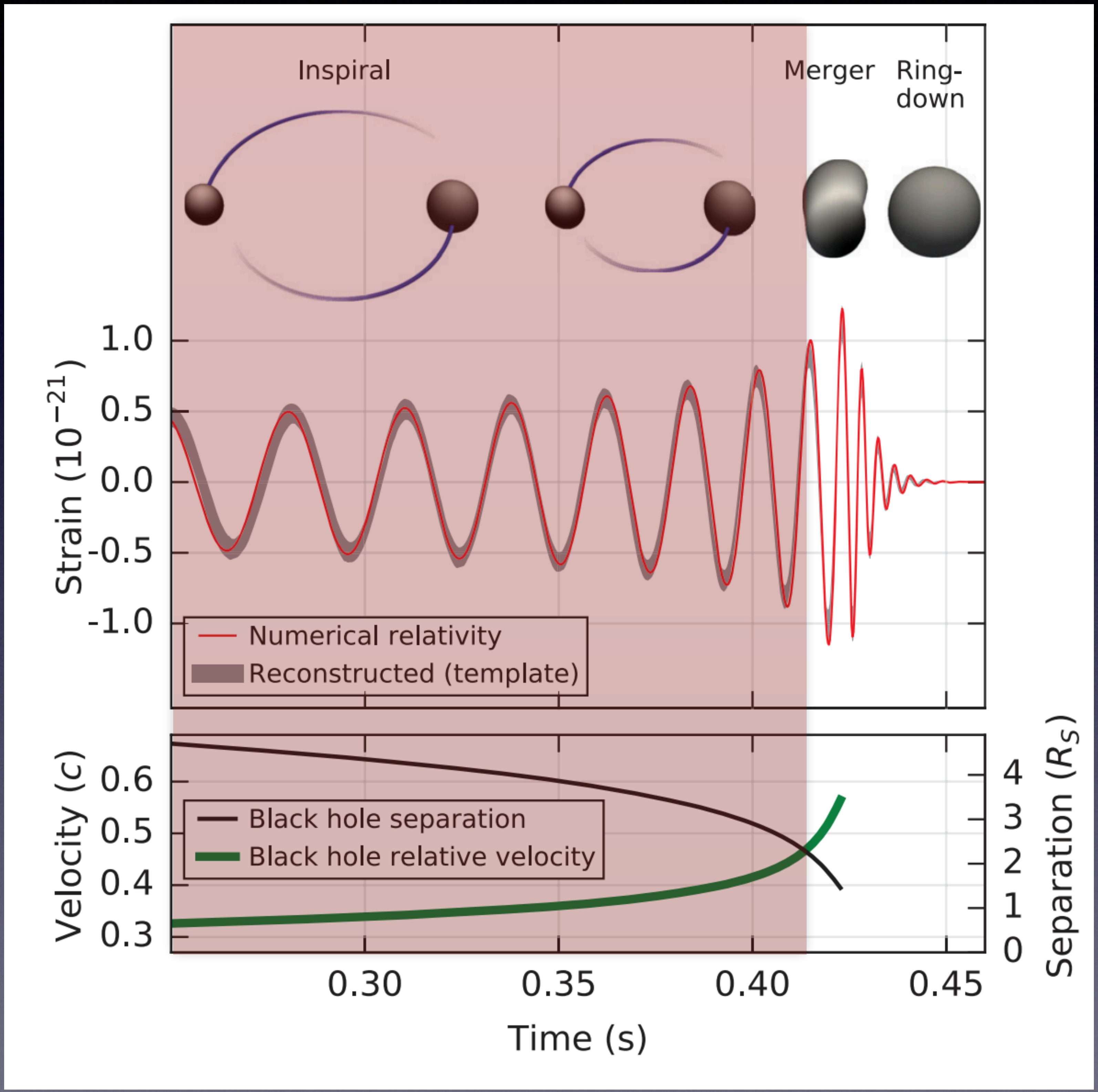

LSC collaboration 2015

The ISCO

Geodesics in Schwarzschild/Kerr separate

$$\frac{1}{2}\left(\frac{dr}{d\lambda}\right)^2 + V(r, L_z) = \frac{1}{2}E^2$$

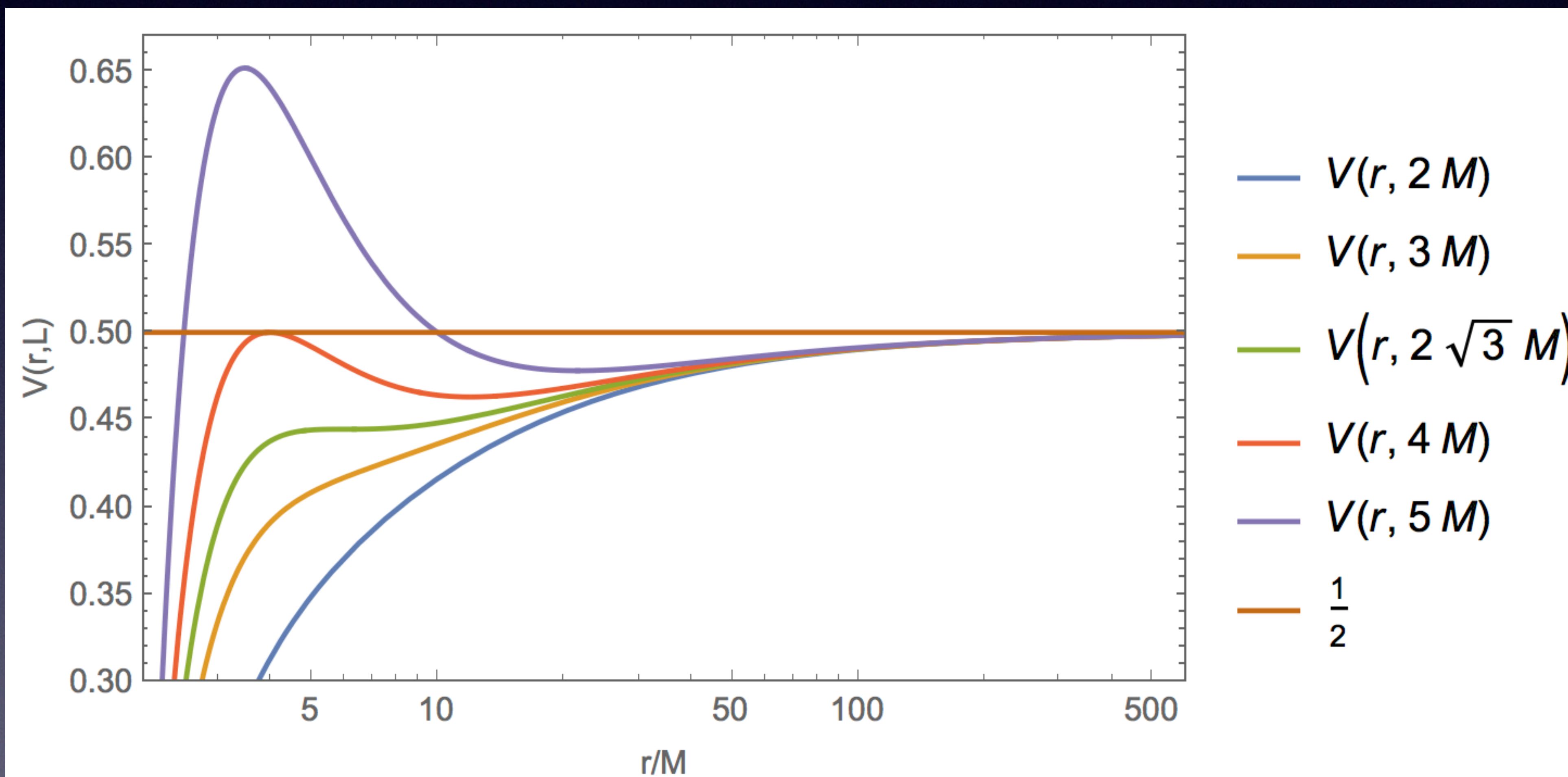

- Schwarzschild ISCO at r=6M
- Different than in Newtonian gravity (circular orbits down to r=0)

The effect of BH spins: frame-dragging in isolated BHs

Spin affects motion around BHs (“frame dragging”), e.g. ISCO position depends on spin

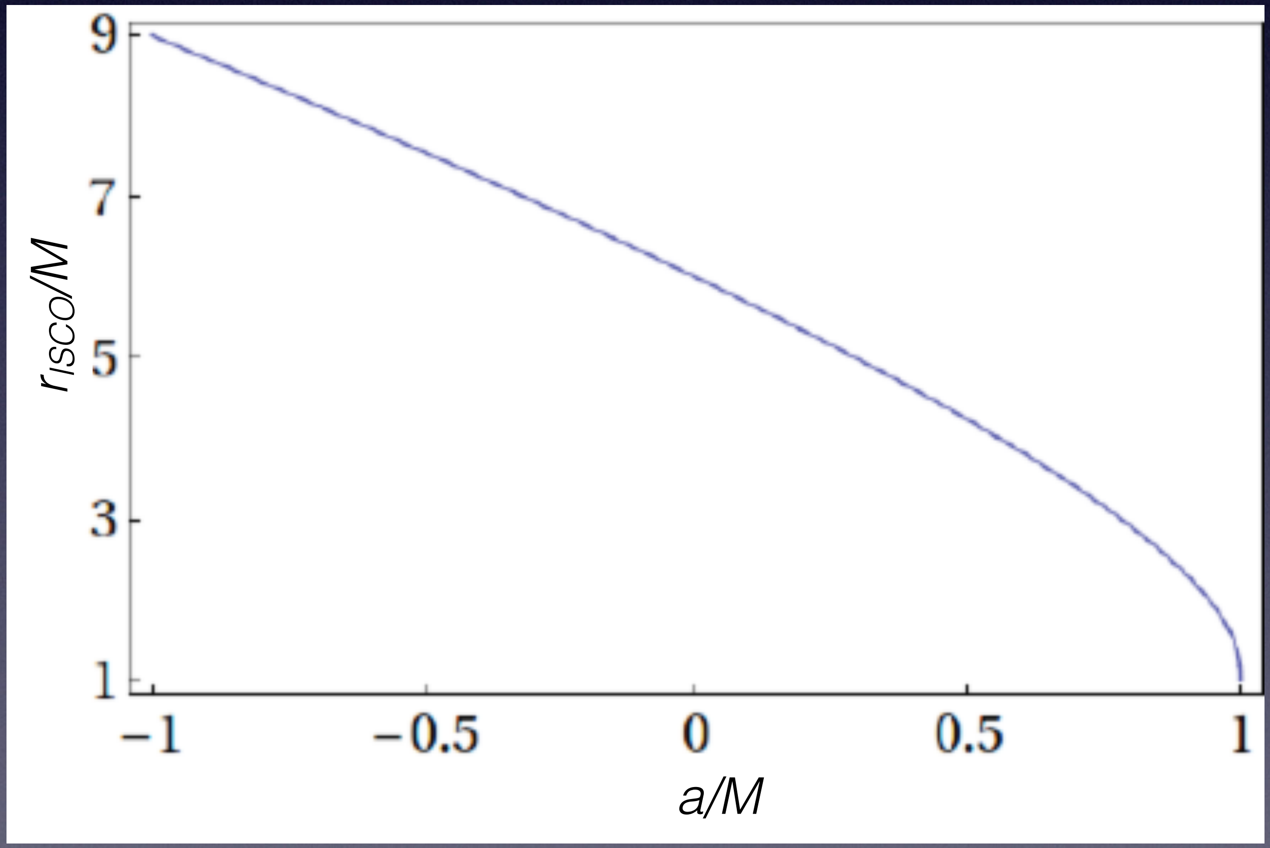

ISCO = inner edge of thin disks

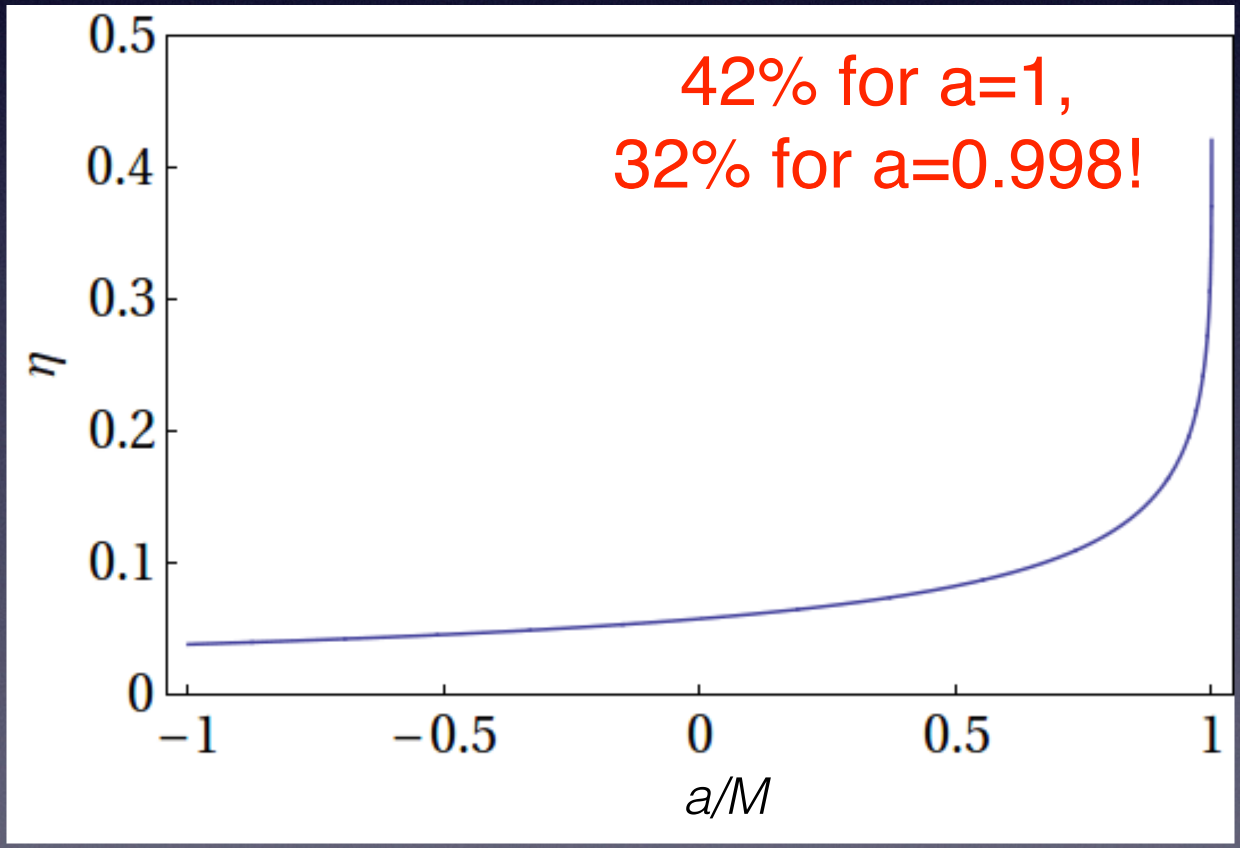

Efficiency of EM emission from thin disks

EM BH spin measurements

Continuum fitting/iron-Kα lines

Binary System	$M/M_\odot$	a	Reference
4U 1543-47	9.4 ± 1.0	$0.75 - 0.85$	Shafee et al. (2006)
GRO J1655-40	6.30 ± 0.27	$0.65 - 0.75$	Shafee et al. (2006)
GRS 1915+105	14.0 ± 4.4	> 0.98	McClintock et al. (2006)
LMC X-3	$5 - 11$	< 0.26	Davis et al. (2006)
M33 X-7	15.65 ± 1.45	0.84 ± 0.05	Liu et al. (2008, 2010)
LMC X-1	10.91 ± 1.41	$0.92^{+0.05}_{-0.07}$	Gou et al. (2009)
XTE J1550-564	9.10 ± 0.61	$0.34^{+0.20}_{-0.28}$	Steiner et al. (2010b)

Stellar-mass BH spins

Object name	Galaxy type	z	L_X[erg s^{-1}]	$f_{\rm Edd}$	$\log(M_{\rm bh}[M_\odot])$	spin
1H0707-495	–	0.0411	3.7×10^{43}	1.0	6.70 ± 0.4	> 0.97
Mrk1018	S0	0.043	9.0×10^{43}	0.01	8.15	$0.58^{+0.36}_{-0.74}$
NGC4051	SAB(rs)bc	0.0023	3.0×10^{42}	0.03	6.28	> 0.99
NGC3783	SB(r)ab	0.0097	1.8×10^{44}	0.06	7.47 ± 0.08	> 0.88
1H0419-577	–	0.104	1.8×10^{44}	0.04	8.18 ± 0.05	> 0.89
3C120	S0	0.033	2.0×10^{44}	0.31	$7.74^{+0.20}_{-0.22}$	> 0.95
MCG-6-30-15	E/S0	0.008	1.0×10^{43}	0.4	6.65 ± 0.17	> 0.98
Ark564	SB	0.0247	1.4×10^{44}	0.11	< 6.90	$0.96^{+0.01}_{-0.06}$
TonS180	–	0.062	3.0×10^{44}	2.15	$7.30^{+0.60}_{-0.40}$	$0.91^{+0.02}_{-0.09}$
RBS1124	–	0.208	1.0×10^{45}	0.15	8.26	> 0.97
Mrk110	–	0.0355	1.8×10^{44}	0.16	7.40 ± 0.09	> 0.89
Mrk841	E	0.0365	8.0×10^{43}	0.44	7.90	> 0.52
Fairall9	Sc	0.047	3.0×10^{44}	0.05	8.41 ± 0.11	$0.52^{+0.19}_{-0.15}$
SWIFTJ2127.4+5654	SB0/a(s)	0.0147	1.2×10^{43}	0.18	7.18 ± 0.07	0.6 ± 0.2
Mrk79	SBb	0.0022	4.7×10^{43}	0.05	7.72 ± 0.14	0.7 ± 0.1
Mrk335	S0a	0.026	5.0×10^{43}	0.25	7.15 ± 0.13	$0.83^{+0.09}_{-0.13}$
Ark120	Sb/pec	0.0327	3.0×10^{45}	1.27	8.18 ± 0.12	$0.64^{+0.19}_{-0.11}$
Mrk359	pec	0.0174	6.0×10^{42}	0.25	6.04	$0.66^{+0.30}_{-0.54}$
IRAS13224-3809	–	0.0667	7.0×10^{43}	0.71	7.00	> 0.987
NGC1365	SB(s)b	0.0054	2.7×10^{42}	0.06	$6.60^{+1.40}_{-0.30}$	$0.97^{+0.01}_{-0.04}$

Compilations (Reynolds, Brenneman,...)
of massive BH spins

Frame-dragging in binaries

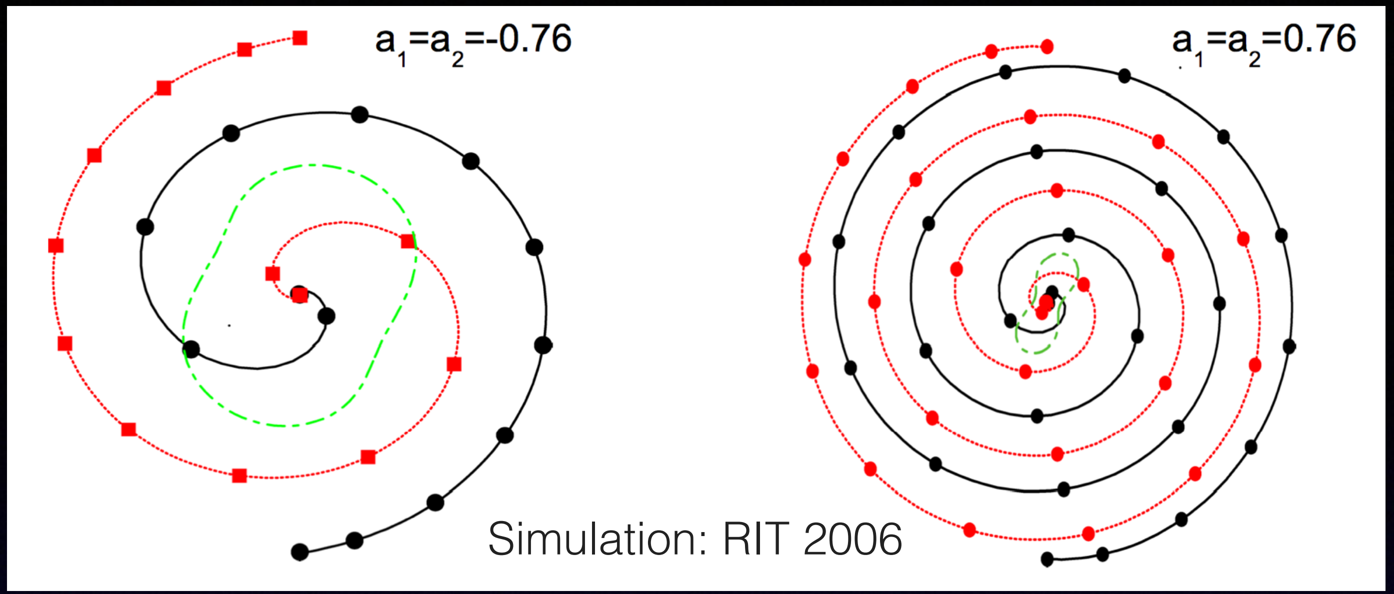

- For large spins aligned with L, effective ISCO moves inward …

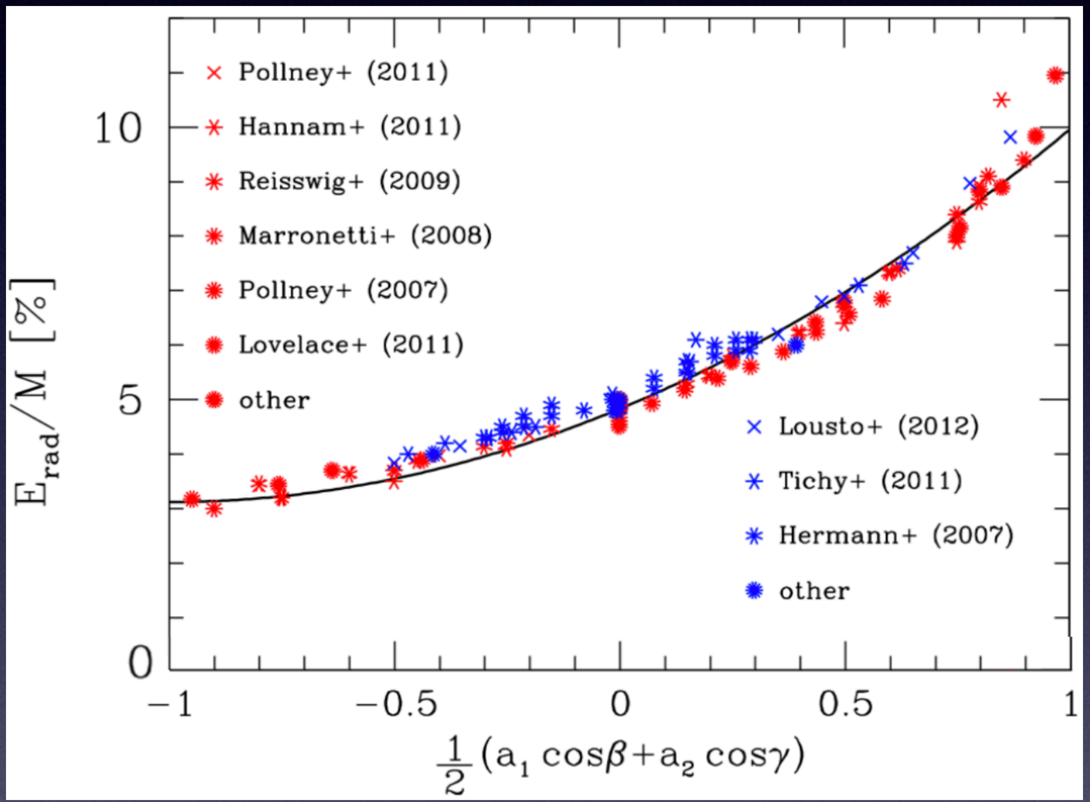

EB, Morozova & Rezzolla (2012)

- ... and GW "efficiency" gets larger (spins increase GW amplitude)

- Spin-orbit and spin-spin precession

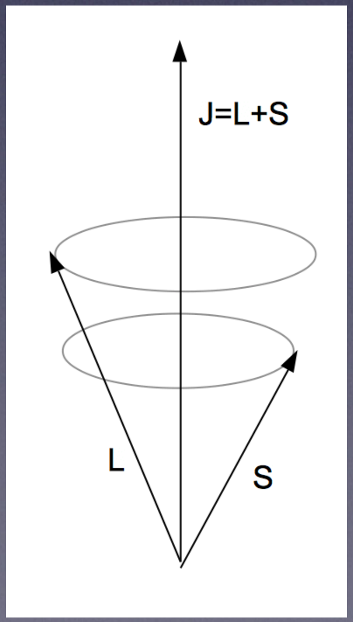

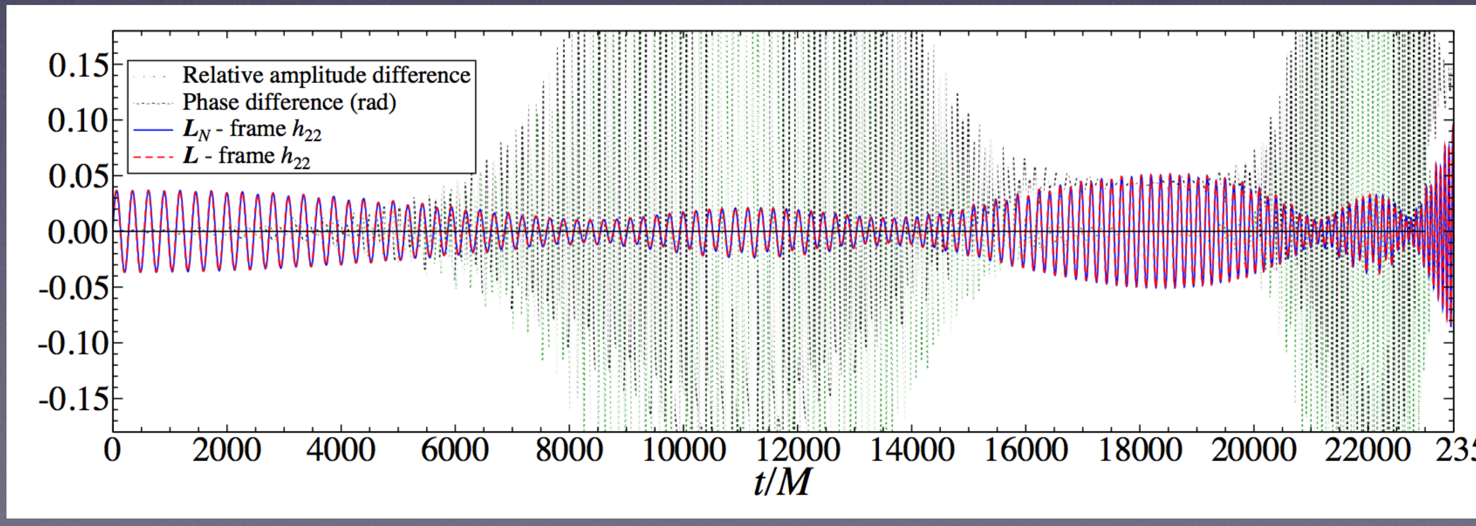

EOB waveform, UMD/AEI group

Beyond geodesics: the PN expansion

Expand binary dynamics in powers of v/c [$(v/c)^{2n}$ = nPN]

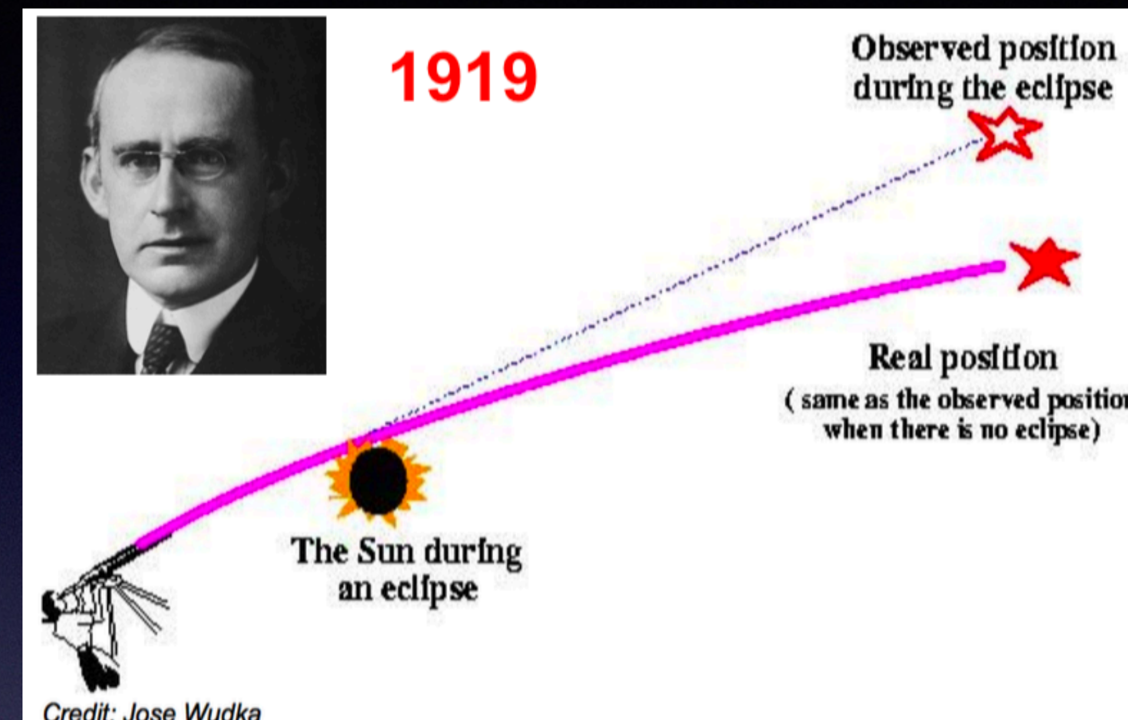

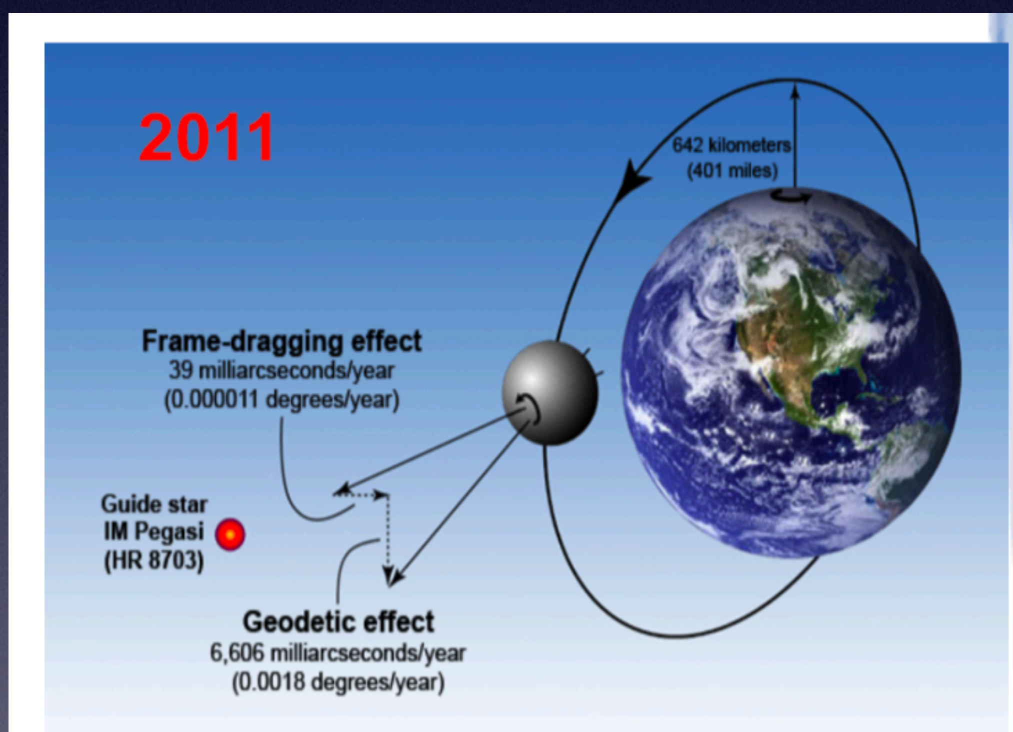

	Measured	Predicted
Geodetic precession (mas)	6602 ± 18	6606
Frame-dragging (mas)	37.2 ± 7.2	39.2

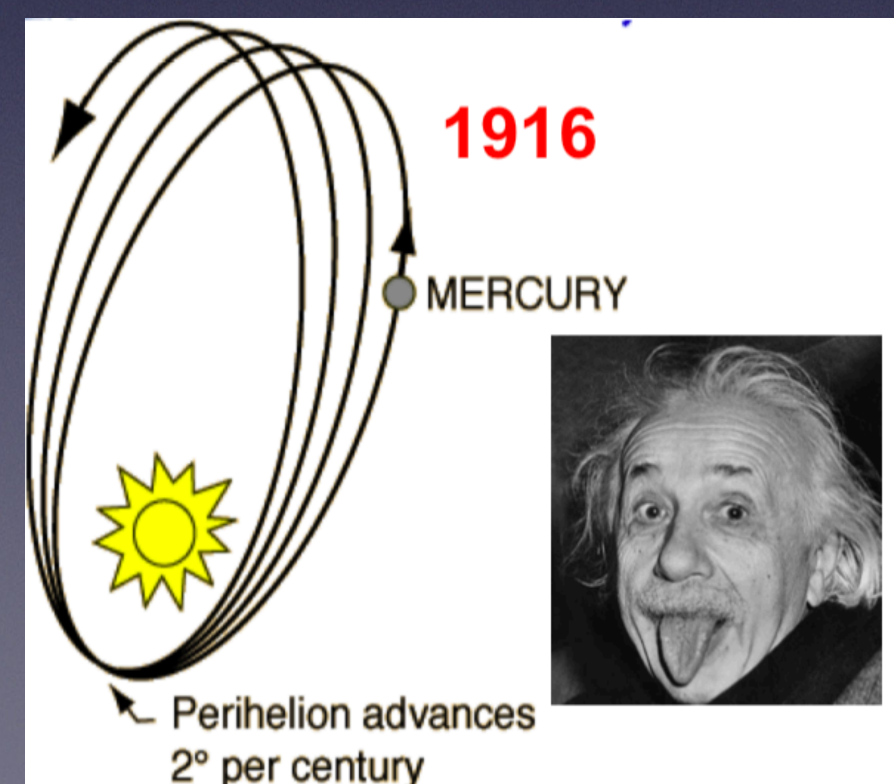

The PN Hamiltonian

$$H = m_1c^2 + m_2c^2 + H_N + H_{1PN} + H_{2PN} + H_{3PN} + \ldots$$

$$\hat{H} = (H - Mc^2)/\mu \qquad M = m_1 + m_2$$

$$\mu = m_1m_2/M \qquad \nu = \mu/M$$

$$p_r = (\mathbf{n}\cdot\mathbf{p}),\ \mathbf{q} = (\mathbf{x}_1 - \mathbf{x}_2)/GM,$$

$$\mathbf{p} = \mathbf{p}_1/\mu,\ r = r_{12} = |\mathbf{x}_1 - \mathbf{x}_2|,$$

$$\mathbf{n} = \mathbf{q}/|\mathbf{q}| \qquad \mathbf{p}_1 + \mathbf{p}_2 = 0$$

$$H^{1PN}_{\mathrm{S_1S_2}} = \frac{G}{c^2}\sum_a\sum_{b\neq a}\frac{1}{2r_{ab}^3}\left[3(\mathbf{S}_a\cdot\mathbf{n}_{ab})(\mathbf{S}_b\cdot\mathbf{n}_{ab}) - (\mathbf{S}_a\cdot\mathbf{S}_b)\right]$$

$$H^{1PN}_{\mathrm{SO}} = \frac{G}{c^2}\sum_a\sum_{b\neq a}\frac{1}{r_{ab}^2}(\mathbf{S}_a\times\mathbf{n}_{ab})\cdot\left[\frac{3m_b}{2m_a}\mathbf{p}_a - 2\mathbf{p}_b\right]$$

$$\begin{aligned}
\hat{H}_N &= \frac{p^2}{2} - \frac{1}{q},\\
c^2\hat{H}_{1PN} &= \frac{1}{8}(3\nu-1)p^4 - \frac{1}{2}\left[(3+\nu)p^2 + \nu p_r^2\right]\frac{1}{q} + \frac{1}{2q^2},\\
c^4\hat{H}_{2PN} &= \frac{1}{16}(1-5\nu+5\nu^2)p^6\\
&+ \frac{1}{8}\left[(5-20\nu-3\nu^2)p^4 - 2\nu^2p_r^2p^2 - 3\nu^2p_r^4\right]\frac{1}{q}\\
&+ \frac{1}{2}\left[(5+8\nu)p^2 + 3\nu p_r^2\right]\frac{1}{q^2} - \frac{1}{4}(1+3\nu)\frac{1}{q^3},\\
c^6\hat{H}_{3PN} &= \frac{1}{128}(-5+35\nu-70\nu^2+35\nu^3)p^8\\
&+ \frac{1}{16}\Big[(-7+42\nu-53\nu^2-5\nu^3)p^6 + (2-3\nu)\nu^2p_r^2p^4\\
&\qquad + 3(1-\nu)\nu^2p_r^4p^2 - 5\nu^3p_r^6\Big]\frac{1}{q}\\
&+ \Big[\frac{1}{16}(-27+136\nu+109\nu^2)p^4 + \frac{1}{16}(17+30\nu)\nu p_r^2p^2\\
&\qquad + \frac{1}{12}(5+43\nu)\nu p_r^4\Big]\frac{1}{q^2}\\
&+ \Big[\left(-\frac{25}{8} + \left(\frac{1}{64}\pi^2 - \frac{335}{48}\right)\nu - \frac{23}{8}\nu^2\right)p^2\\
&\qquad + \left(-\frac{85}{16} - \frac{3}{64}\pi^2 - \frac{7}{4}\nu\right)\nu p_r^2\Big]\frac{1}{q^3}\\
&+ \left[\frac{1}{8} + \left(\frac{109}{12} - \frac{21}{32}\pi^2\right)\nu\right]\frac{1}{q^4}.
\end{aligned}$$

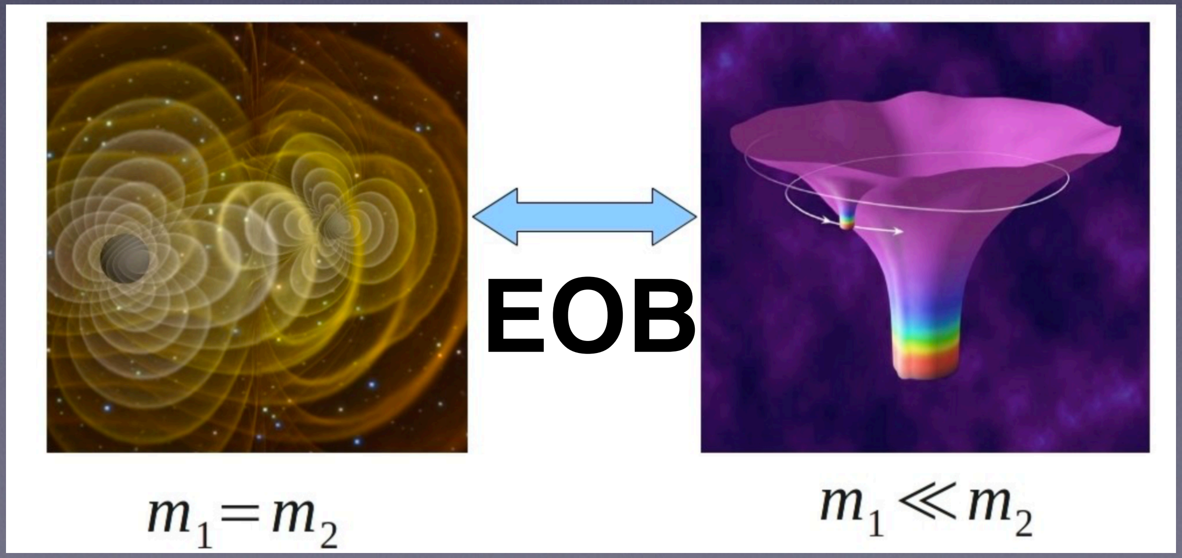

Dynamics is qualitatively similar to a particle in Schwarzschild/Kerr (and also semi-quantitatively if particle's mass replaced by reduced mass)

BH binaries inspiral till (effective) ISCO

From energy balance: $$\frac{\dot{P}_b}{P_b} = -\frac{3}{2}\frac{\dot{E}_b}{E_b}$$

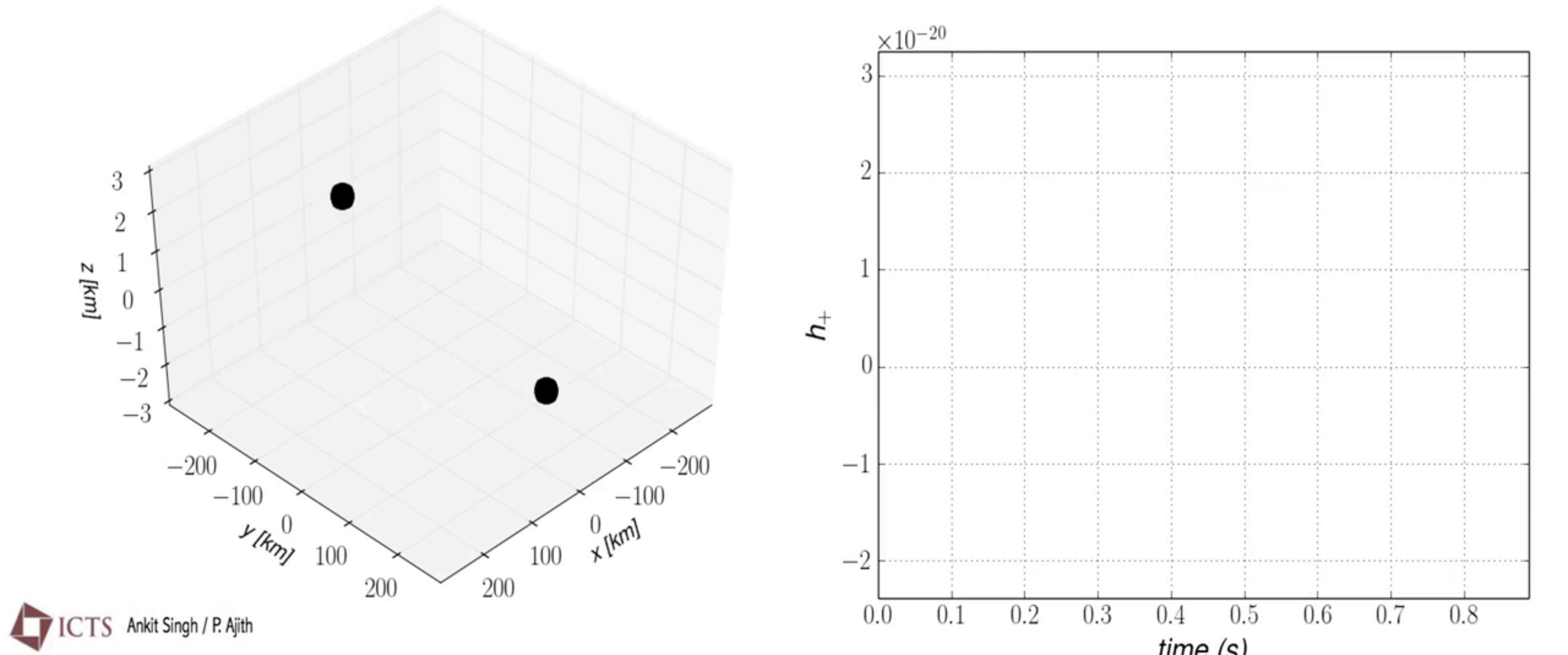

Extracting BH masses

$$\mathcal{M} = \frac{(m_1 m_2)^{3/5}}{(m_1+m_2)^{1/5}} = \frac{c^3}{G}\left[\frac{5}{96}\pi^{-8/3} f^{-11/3}\dot{f}\right]^{3/5}$$

$\rightarrow$ $\mathcal{M} \simeq 30 M_\odot$

$\rightarrow$ $M = m_1 + m_2 \gtrsim 70 M_\odot$

$\rightarrow$ $2GM/c^2 \gtrsim 210$ km

f_{gw}~ 75 Hz corresponds to r_{12}~350 km

Objects in GW150914 must be BHs (not WDs or NSs)

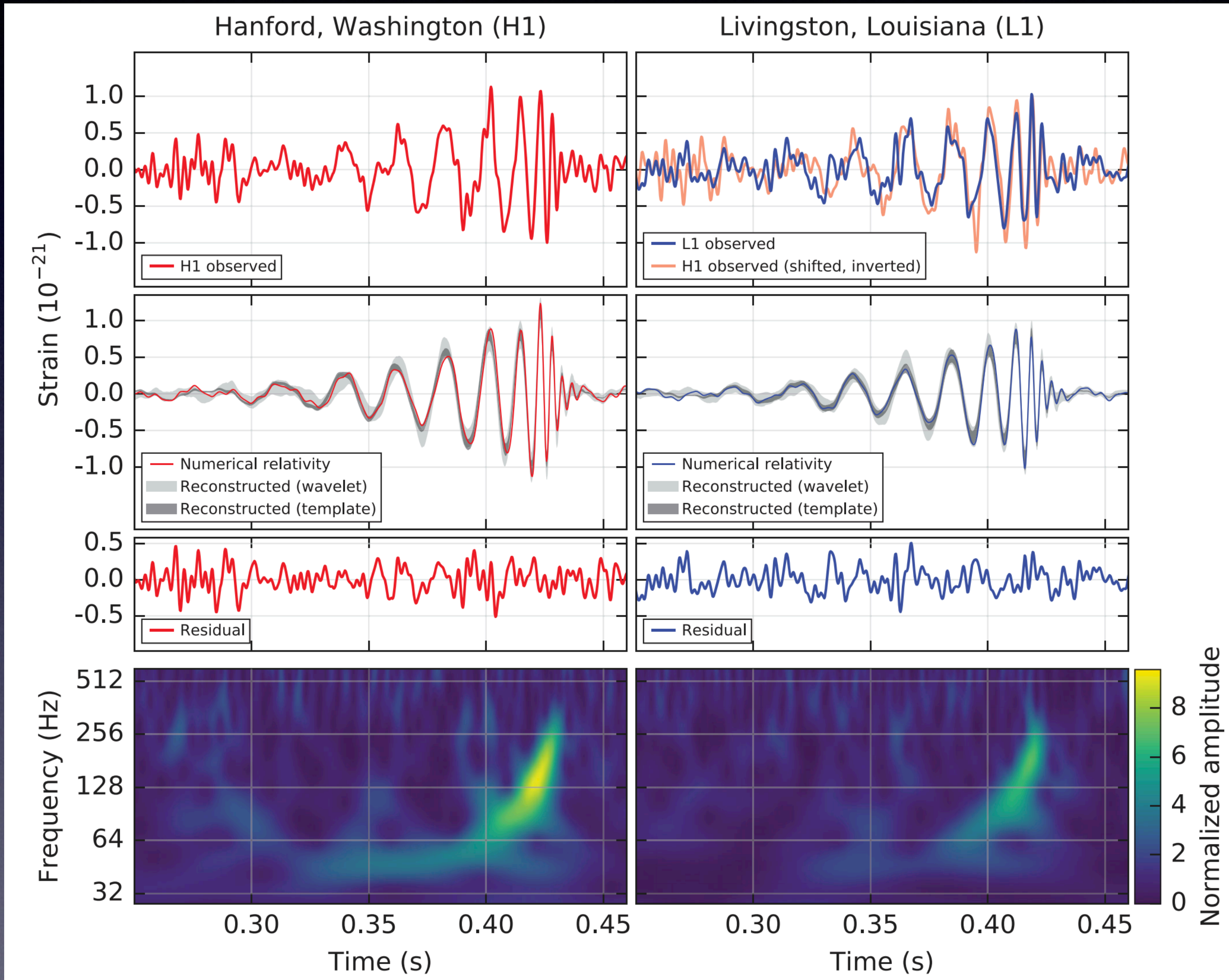

LSC collaboration 2015

Extracting the BH masses

Event	$m_1/\mathrm{M}_\odot$	$m_2/\mathrm{M}_\odot$	$\mathcal{M}/\mathrm{M}_\odot$	χ_{eff}	$M_{\mathrm{f}}/\mathrm{M}_\odot$	a_{f}	$E_{\mathrm{rad}}/(\mathrm{M}_\odot c^2)$	$\ell_{\mathrm{peak}}/(\mathrm{erg\,s}^{-1})$	d_L/Mpc	z	$\Delta\Omega/\mathrm{deg}^2$
GW150914	$35.6^{+4.8}_{-3.0}$	$30.6^{+3.0}_{-4.4}$	$28.6^{+1.6}_{-1.5}$	$-0.01^{+0.12}_{-0.13}$	$63.1^{+3.3}_{-3.0}$	$0.69^{+0.05}_{-0.04}$	$3.1^{+0.4}_{-0.4}$	$3.6^{+0.4}_{-0.4} \times 10^{56}$	430^{+150}_{-170}	$0.09^{+0.03}_{-0.03}$	179
GW151012	$23.3^{+14.0}_{-5.5}$	$13.6^{+4.1}_{-4.8}$	$15.2^{+2.0}_{-1.1}$	$0.04^{+0.28}_{-0.19}$	$35.7^{+9.9}_{-3.8}$	$0.67^{+0.13}_{-0.11}$	$1.5^{+0.5}_{-0.5}$	$3.2^{+0.8}_{-1.7} \times 10^{56}$	1060^{+540}_{-480}	$0.21^{+0.09}_{-0.09}$	1555
GW151226	$13.7^{+8.8}_{-3.2}$	$7.7^{+2.2}_{-2.6}$	$8.9^{+0.3}_{-0.3}$	$0.18^{+0.20}_{-0.12}$	$20.5^{+6.4}_{-1.5}$	$0.74^{+0.07}_{-0.05}$	$1.0^{+0.1}_{-0.2}$	$3.4^{+0.7}_{-1.7} \times 10^{56}$	440^{+180}_{-190}	$0.09^{+0.04}_{-0.04}$	1033
GW170104	$31.0^{+7.2}_{-5.6}$	$20.1^{+4.9}_{-4.5}$	$21.5^{+2.1}_{-1.7}$	$-0.04^{+0.17}_{-0.20}$	$49.1^{+5.2}_{-3.9}$	$0.66^{+0.08}_{-0.10}$	$2.2^{+0.5}_{-0.5}$	$3.3^{+0.6}_{-0.9} \times 10^{56}$	960^{+430}_{-410}	$0.19^{+0.07}_{-0.08}$	924
GW170608	$10.9^{+5.3}_{-1.7}$	$7.6^{+1.3}_{-2.1}$	$7.9^{+0.2}_{-0.2}$	$0.03^{+0.19}_{-0.07}$	$17.8^{+3.2}_{-0.7}$	$0.69^{+0.04}_{-0.04}$	$0.9^{+0.0}_{-0.1}$	$3.5^{+0.4}_{-1.3} \times 10^{56}$	320^{+120}_{-110}	$0.07^{+0.02}_{-0.02}$	396
GW170729	$50.6^{+16.6}_{-10.2}$	$34.3^{+9.1}_{-10.1}$	$35.7^{+6.5}_{-4.7}$	$0.36^{+0.21}_{-0.25}$	$80.3^{+14.6}_{-10.2}$	$0.81^{+0.07}_{-0.13}$	$4.8^{+1.7}_{-1.7}$	$4.2^{+0.9}_{-1.5} \times 10^{56}$	2750^{+1350}_{-1320}	$0.48^{+0.19}_{-0.20}$	1033
GW170809	$35.2^{+8.3}_{-6.0}$	$23.8^{+5.2}_{-5.1}$	$25.0^{+2.1}_{-1.6}$	$0.07^{+0.16}_{-0.16}$	$56.4^{+5.2}_{-3.7}$	$0.70^{+0.08}_{-0.09}$	$2.7^{+0.6}_{-0.6}$	$3.5^{+0.6}_{-0.9} \times 10^{56}$	990^{+320}_{-380}	$0.20^{+0.05}_{-0.07}$	340
GW170814	$30.7^{+5.7}_{-3.0}$	$25.3^{+2.9}_{-4.1}$	$24.2^{+1.4}_{-1.1}$	$0.07^{+0.12}_{-0.11}$	$53.4^{+3.2}_{-2.4}$	$0.72^{+0.07}_{-0.05}$	$2.7^{+0.4}_{-0.3}$	$3.7^{+0.4}_{-0.5} \times 10^{56}$	580^{+160}_{-210}	$0.12^{+0.03}_{-0.04}$	87
GW170817	$1.46^{+0.12}_{-0.10}$	$1.27^{+0.09}_{-0.09}$	$1.186^{+0.001}_{-0.001}$	$0.00^{+0.02}_{-0.01}$	≤ 2.8	≤ 0.89	≥ 0.04	$\geq 0.1 \times 10^{56}$	40^{+10}_{-10}	$0.01^{+0.00}_{-0.00}$	16
GW170818	$35.5^{+7.5}_{-4.7}$	$26.8^{+4.3}_{-5.2}$	$26.7^{+2.1}_{-1.7}$	$-0.09^{+0.18}_{-0.21}$	$59.8^{+4.8}_{-3.8}$	$0.67^{+0.07}_{-0.08}$	$2.7^{+0.5}_{-0.5}$	$3.4^{+0.5}_{-0.7} \times 10^{56}$	1020^{+430}_{-360}	$0.20^{+0.07}_{-0.07}$	39
GW170823	$39.6^{+10.0}_{-6.6}$	$29.4^{+6.3}_{-7.1}$	$29.3^{+4.2}_{-3.2}$	$0.08^{+0.20}_{-0.22}$	$65.6^{+9.4}_{-6.6}$	$0.71^{+0.08}_{-0.10}$	$3.3^{+0.9}_{-0.8}$	$3.6^{+0.6}_{-0.9} \times 10^{56}$	1850^{+840}_{-840}	$0.34^{+0.13}_{-0.14}$	1651

LSC 2018, O1+O2 detections

Extracting the BH masses

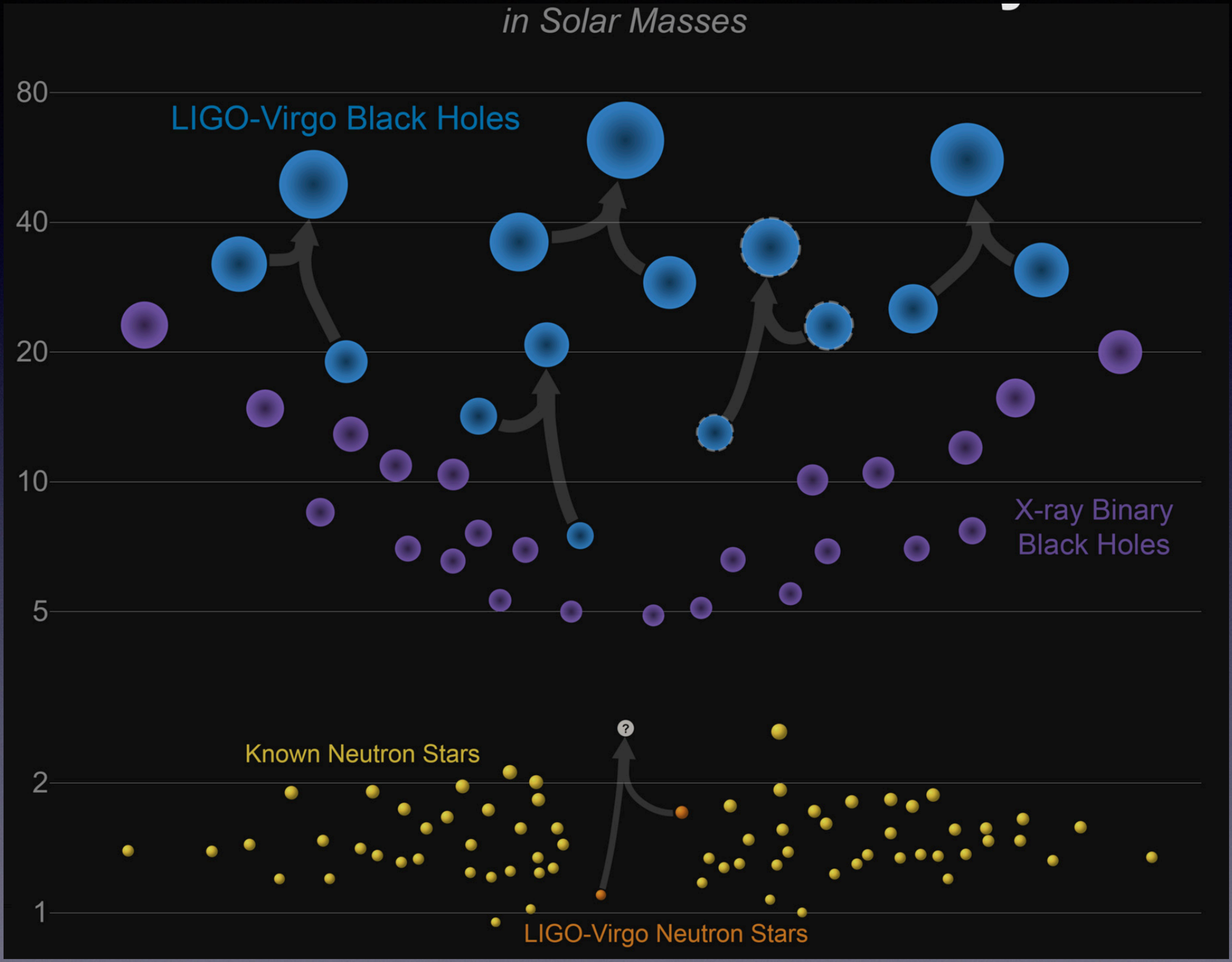

Figure: LSC collaboration 2018

The formation of stellar-mass BHs

- Stellar-mass BH form from massive stars
- Difficult problem: stellar evolution needed to understand mass loss from stellar winds, and explosion mechanism (core collapse SN, direct collapse to BH)
- Evolution depends on mass, metallicity, rotation

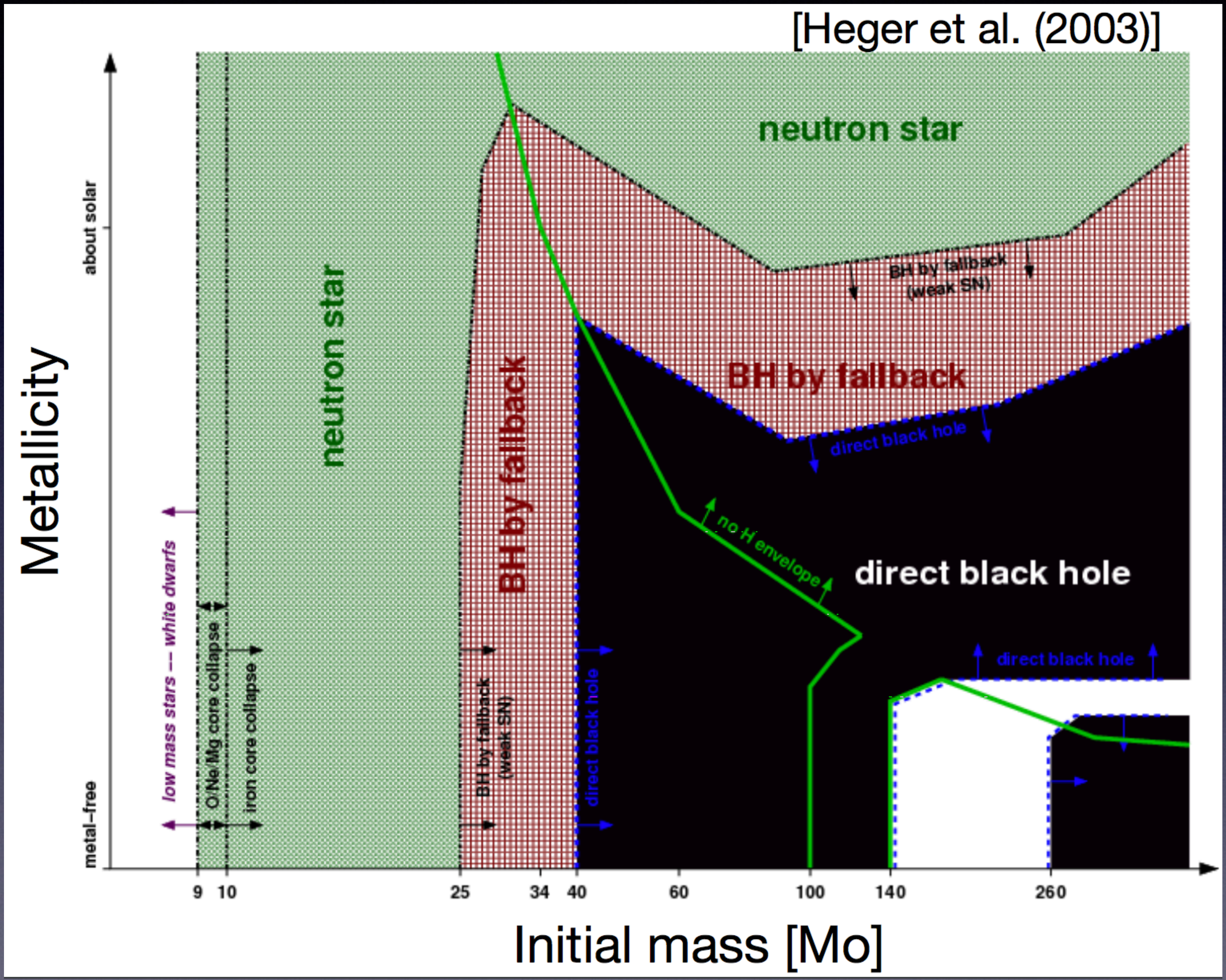

The role of metallicity and stellar winds

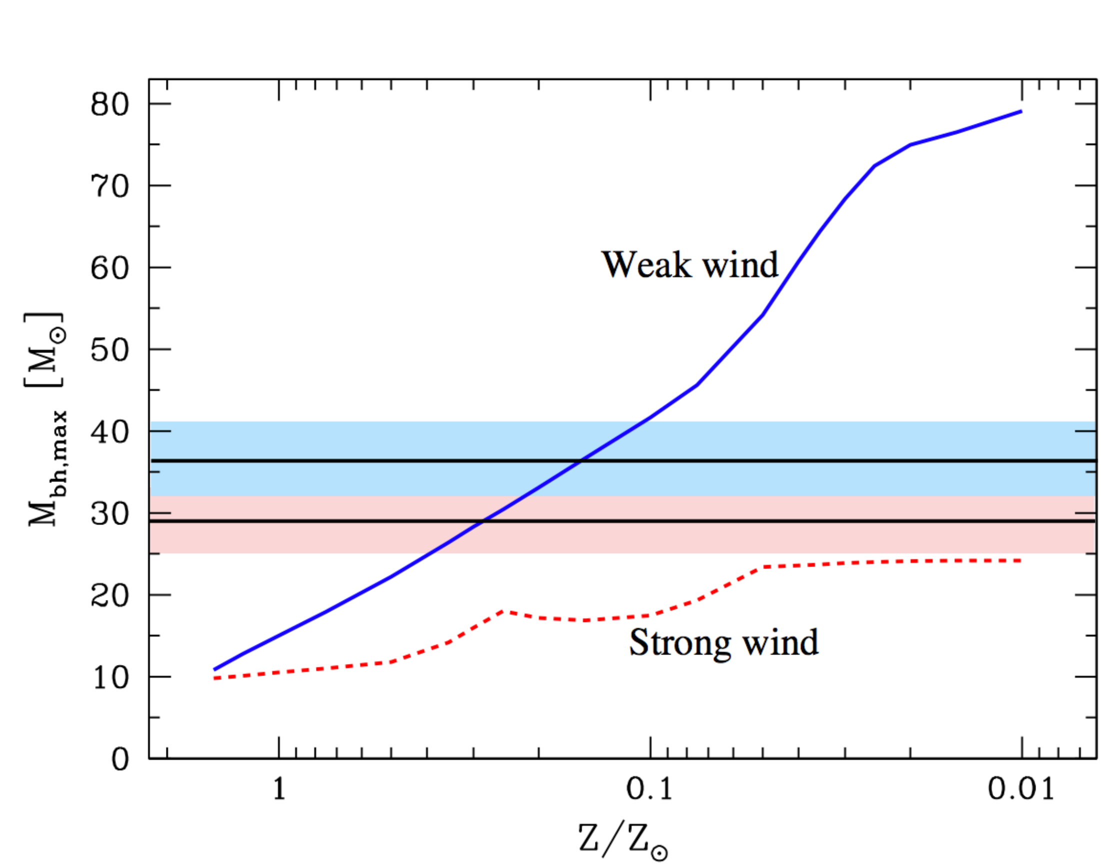

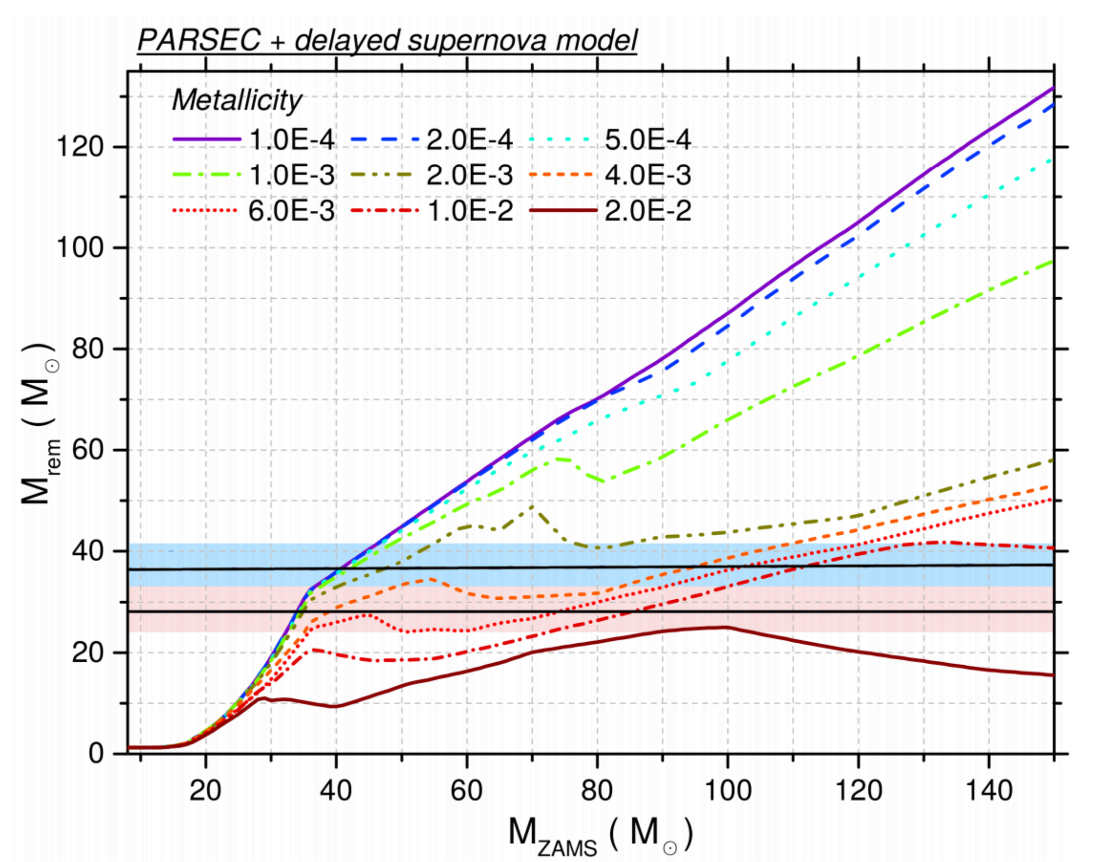

LSC 2015; Belczynski et al 2010; Spera et al 2015

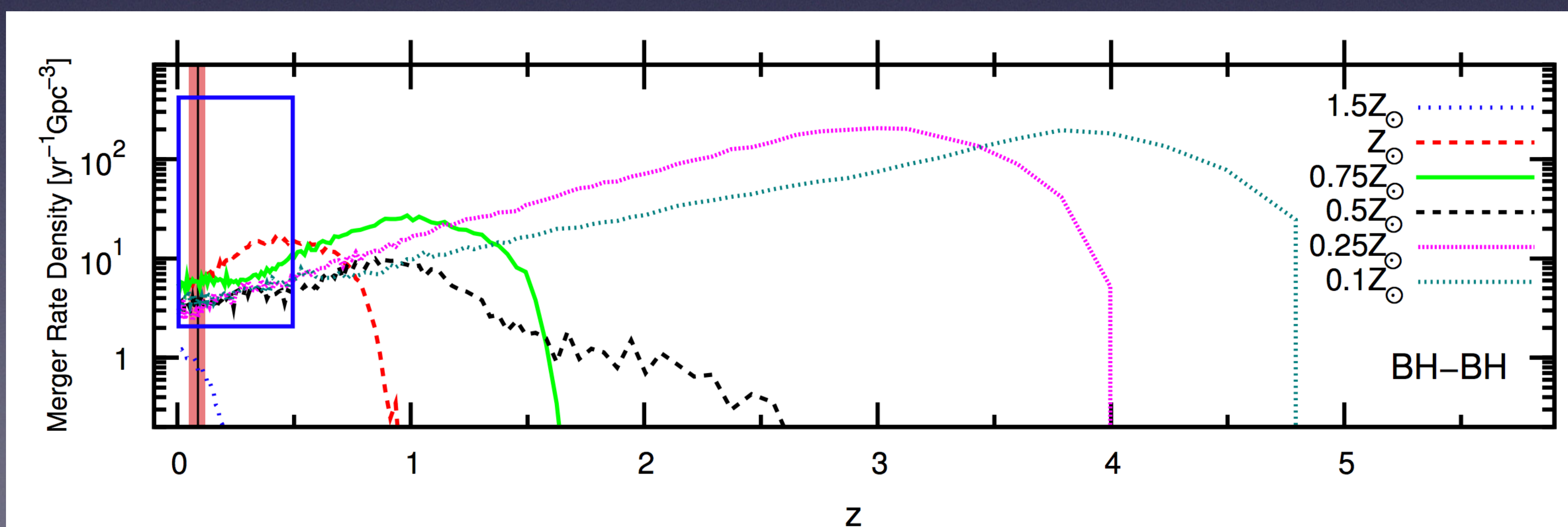

LSC 2015; Dominik et al 2013

The role of metallicity and stellar winds

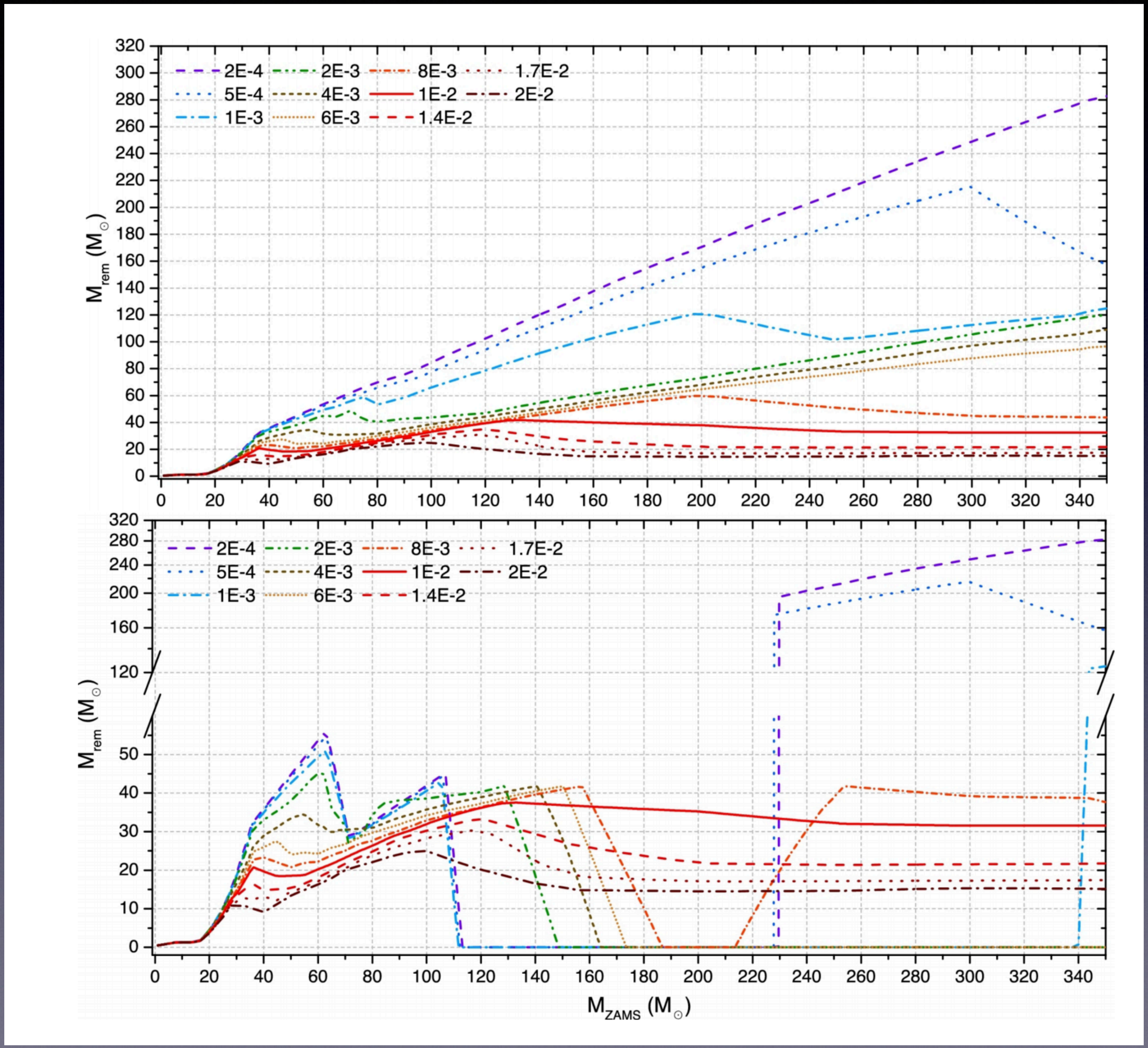

Mapelli 2018;
Spera & Mapelli 2017

Pair instability SN

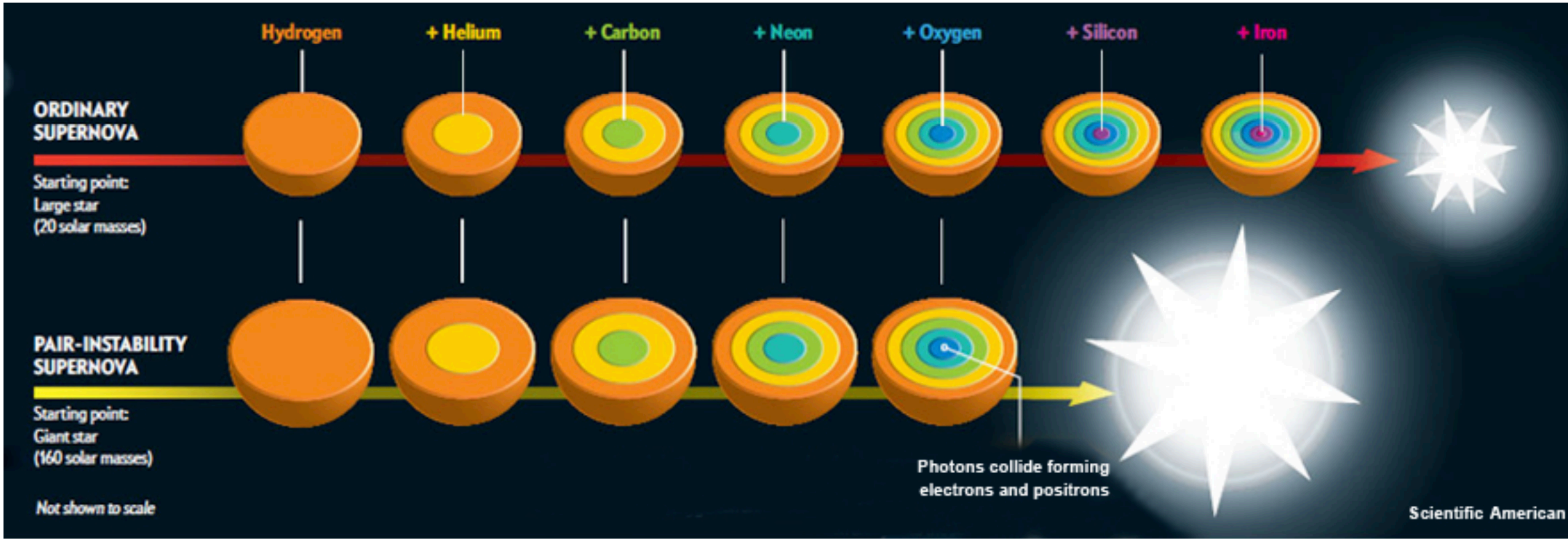

Mass at birth (solar masses)	Helium core mass (solar masses)	Compact remnant	Event
10–95	2–40	Neutron star, black hole	Ordinary supernova
95–130	40–60	Neutron star, black hole	Pulsational pair-instability supernova
130–260	60–137	Explosion, no remnant	Pair-instability supernova
>260	>137	Black hole	?

Woosley, Blinnikov, Heger (2007)

A cutoff at 40 Msun?

Mass at birth (solar masses)	Helium core mass (solar masses)	Compact remnant	Event
10–95	2–40	Neutron star, black hole	Ordinary supernova
95–130	40–60	Neutron star, black hole	Pulsational pair-instability supernova
130–260	60–137	Explosion, no remnant	Pair-instability supernova
>260	>137	Black hole	?

Woosley, Blinnikov, Heger (2007)

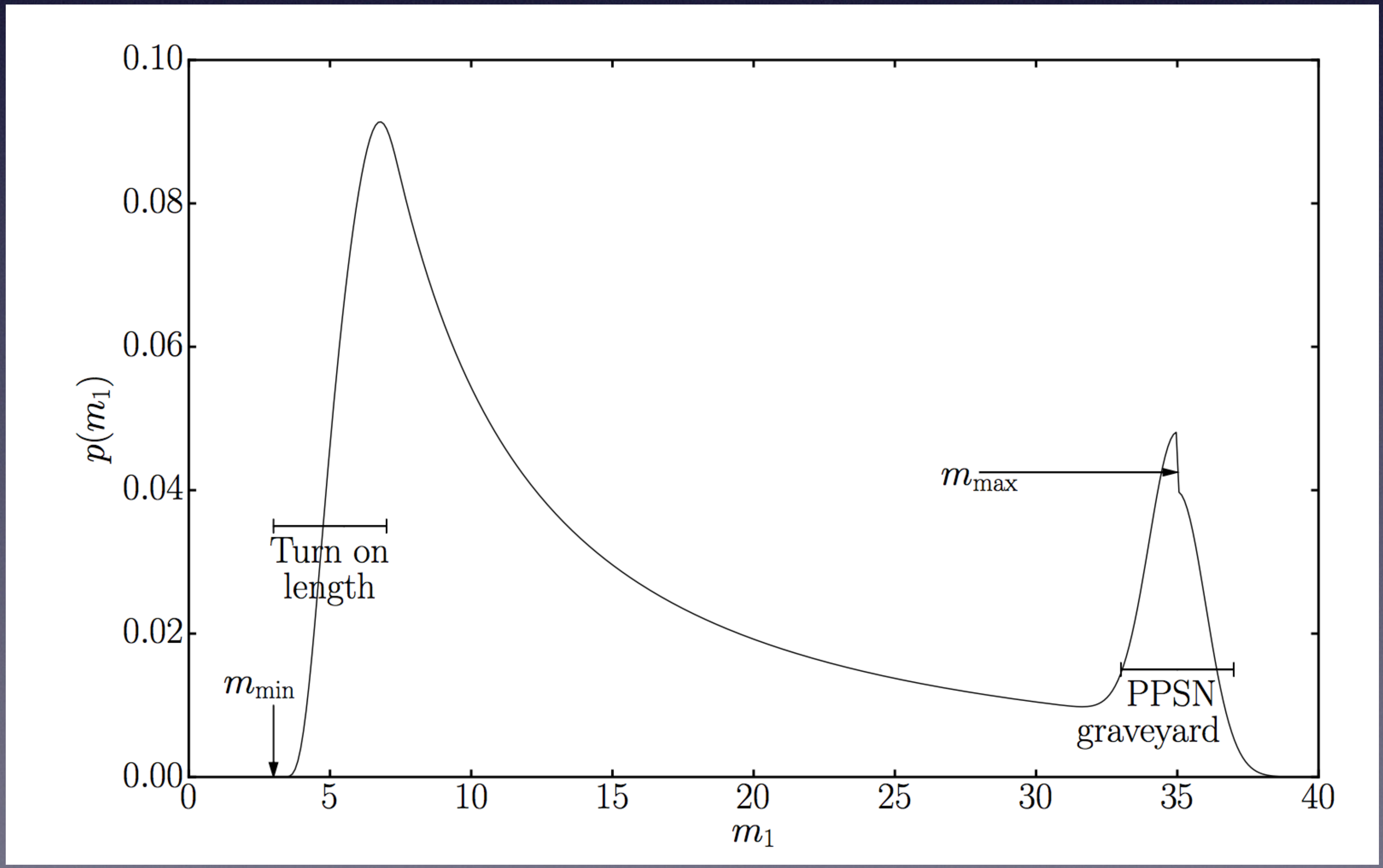

Talbot & Thrane 2018

Updates from O2

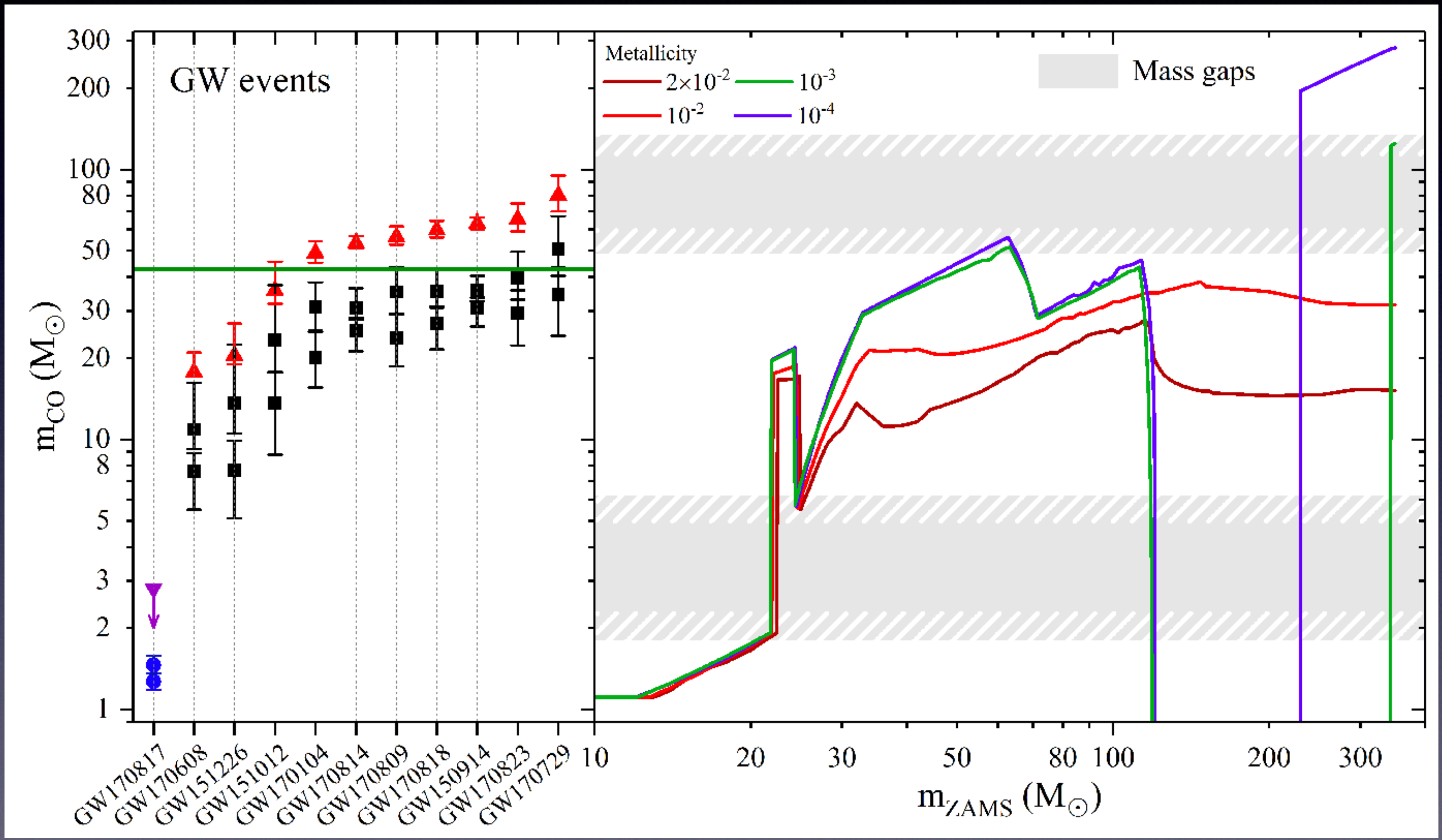

LSC 2018

How do stellar-mass BH *binaries* form?

- In the field (plausible because ~70% of massive stars have companion, c.f. Sana et al 2012)
- In dense environments (globular clusters/nuclear star clusters) via dynamical mechanisms
- Primordial BHs? But problems with CMB/absence of enough MW candidates in radio/X-rays if one wants to explain all of Dark Matter. Formation mechanism also unclear (clustering vs lack of clustering), conflicting predictions for spins

Field BH binaries

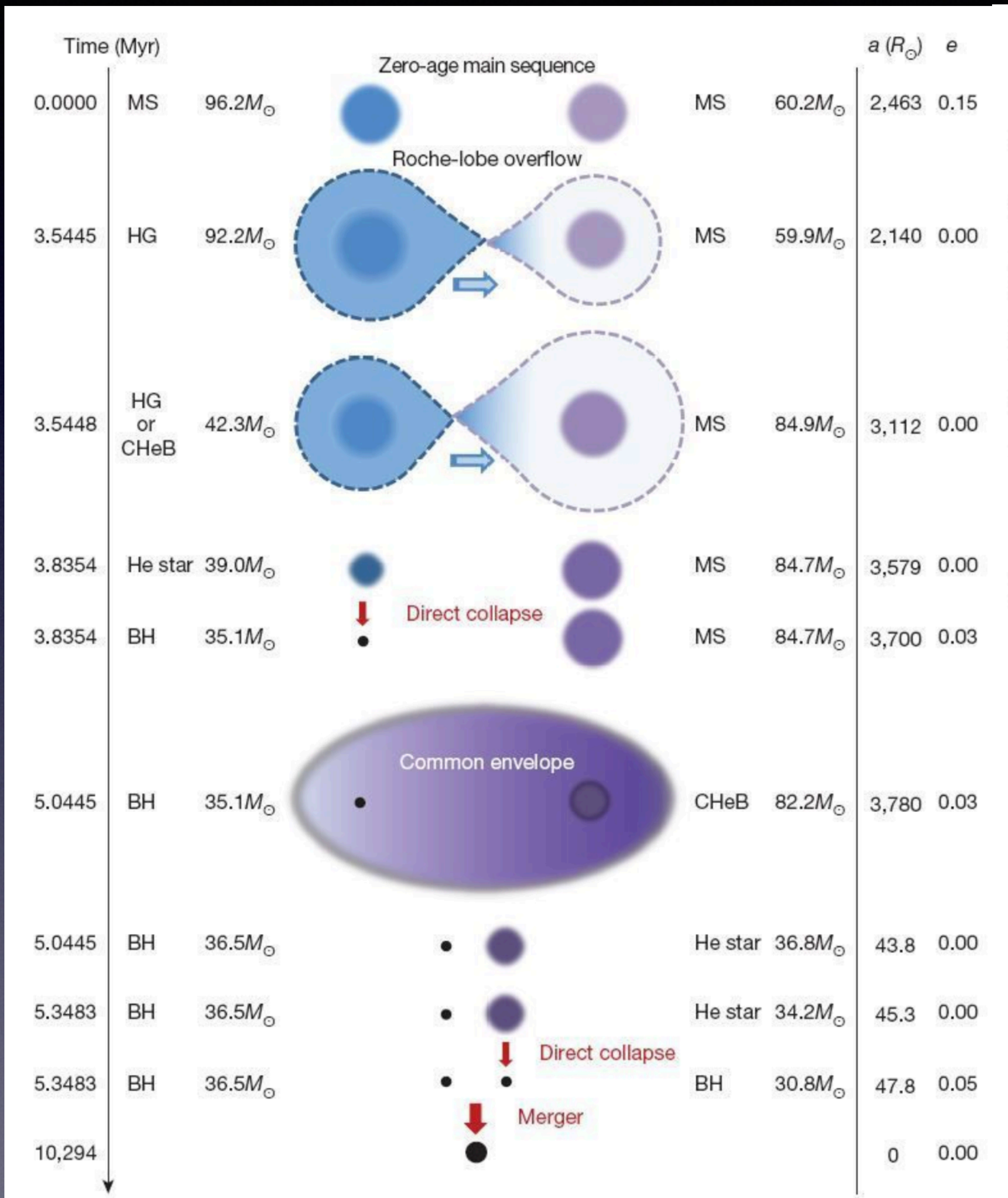

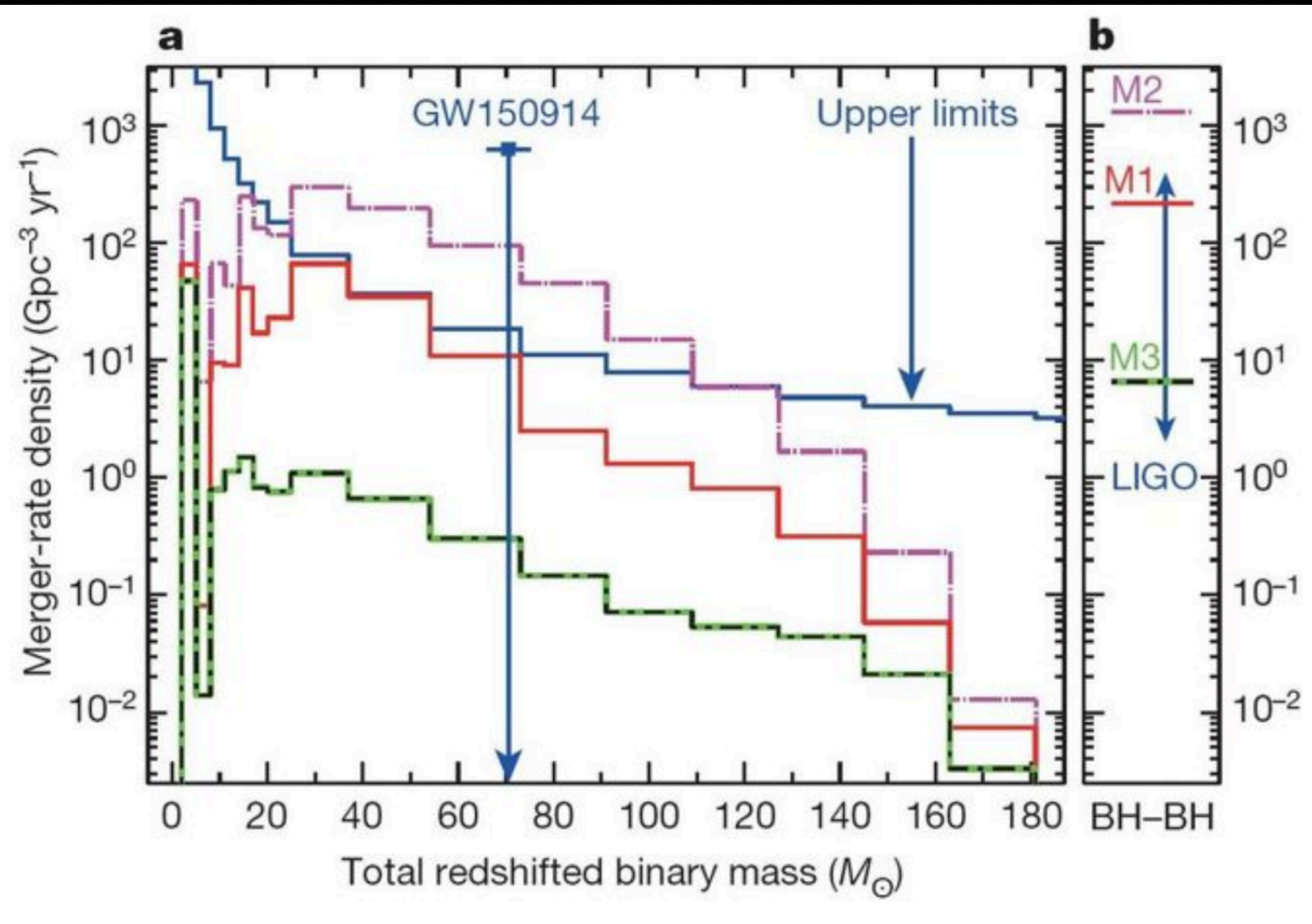

Merger rates for standard model (M1; red); optimistic common-envelope phase (M2; pink); and pessimistic large black-hole kicks (M3; green/black)

Belczynski et al 2016

Field BH binaries

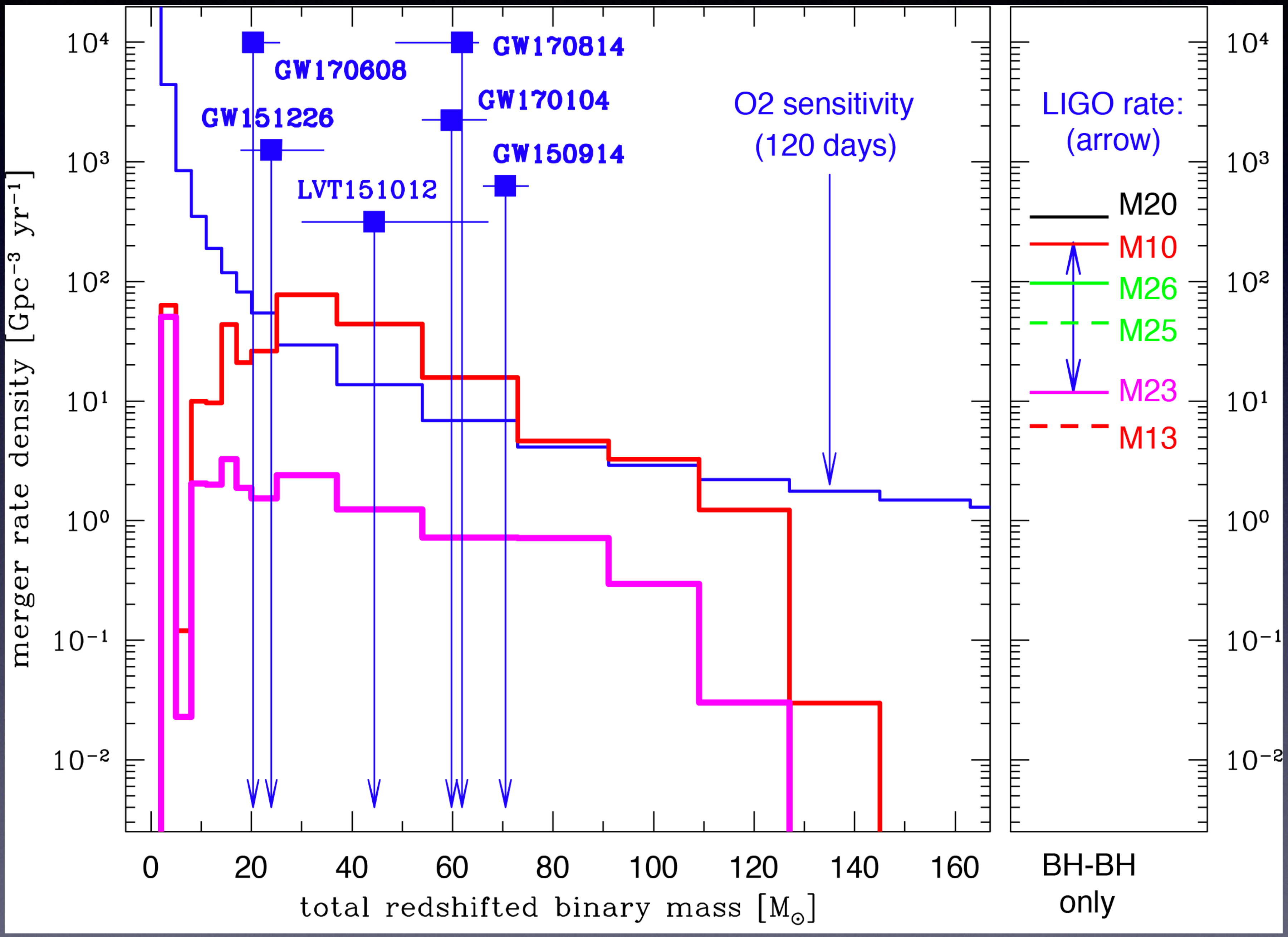

Decreasing natal kicks

From www.syntheticuniverse.org

Dynamical channel

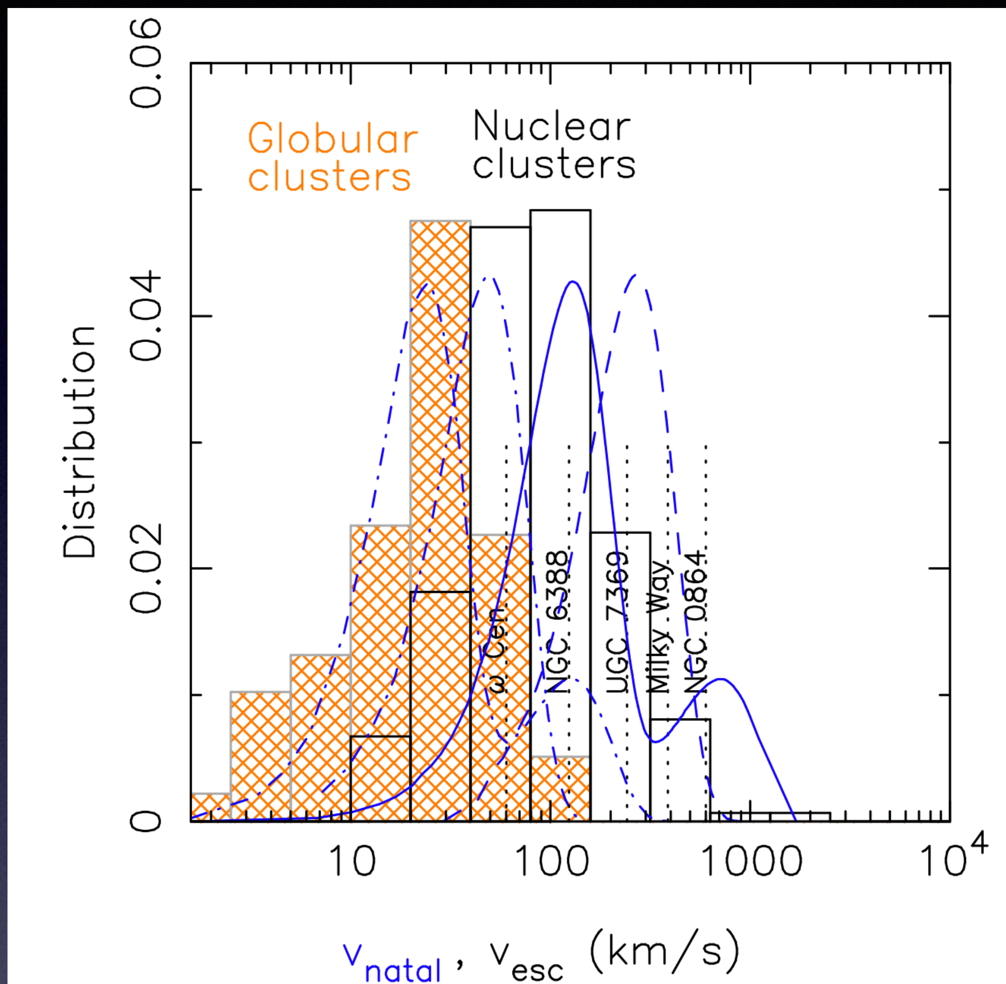

Antonini & Radio 2016

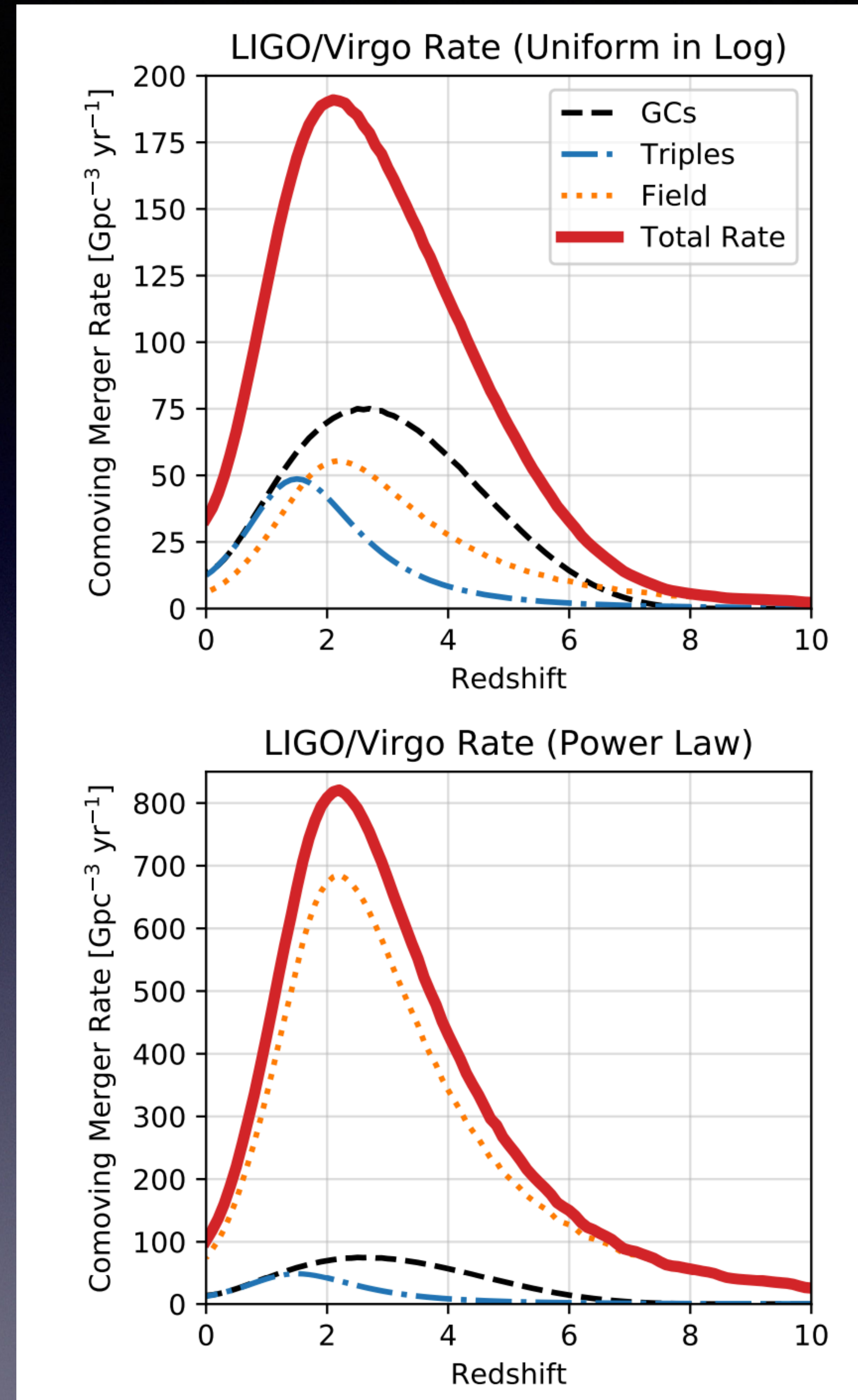

Rodriguez & Loeb 2018

- Similar uncertainties (natal kicks)
- Possible in globular clusters and nuclear star clusters, or even in the field (field triples)
- May be as important as field channel

Extracting BH spins

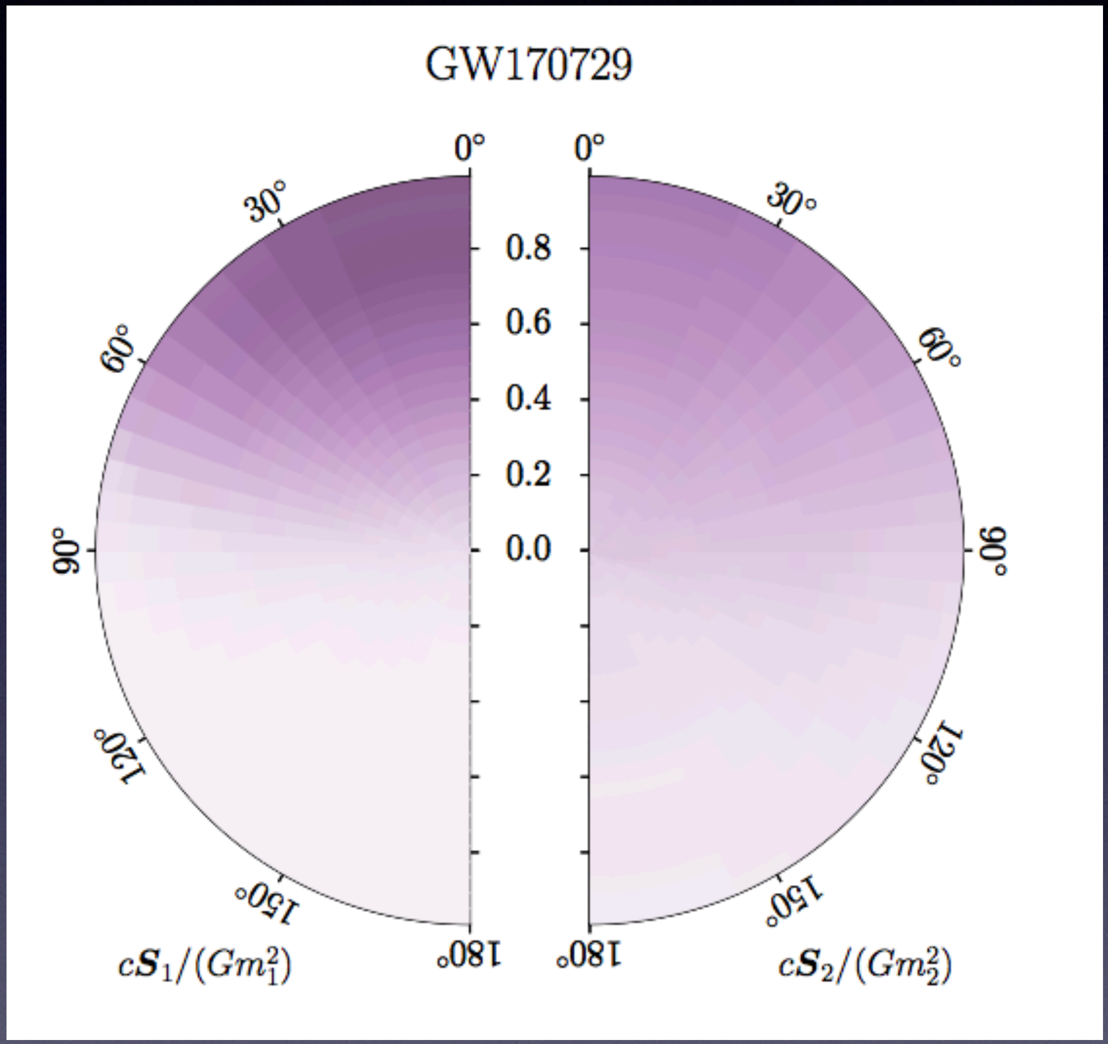

GW170729

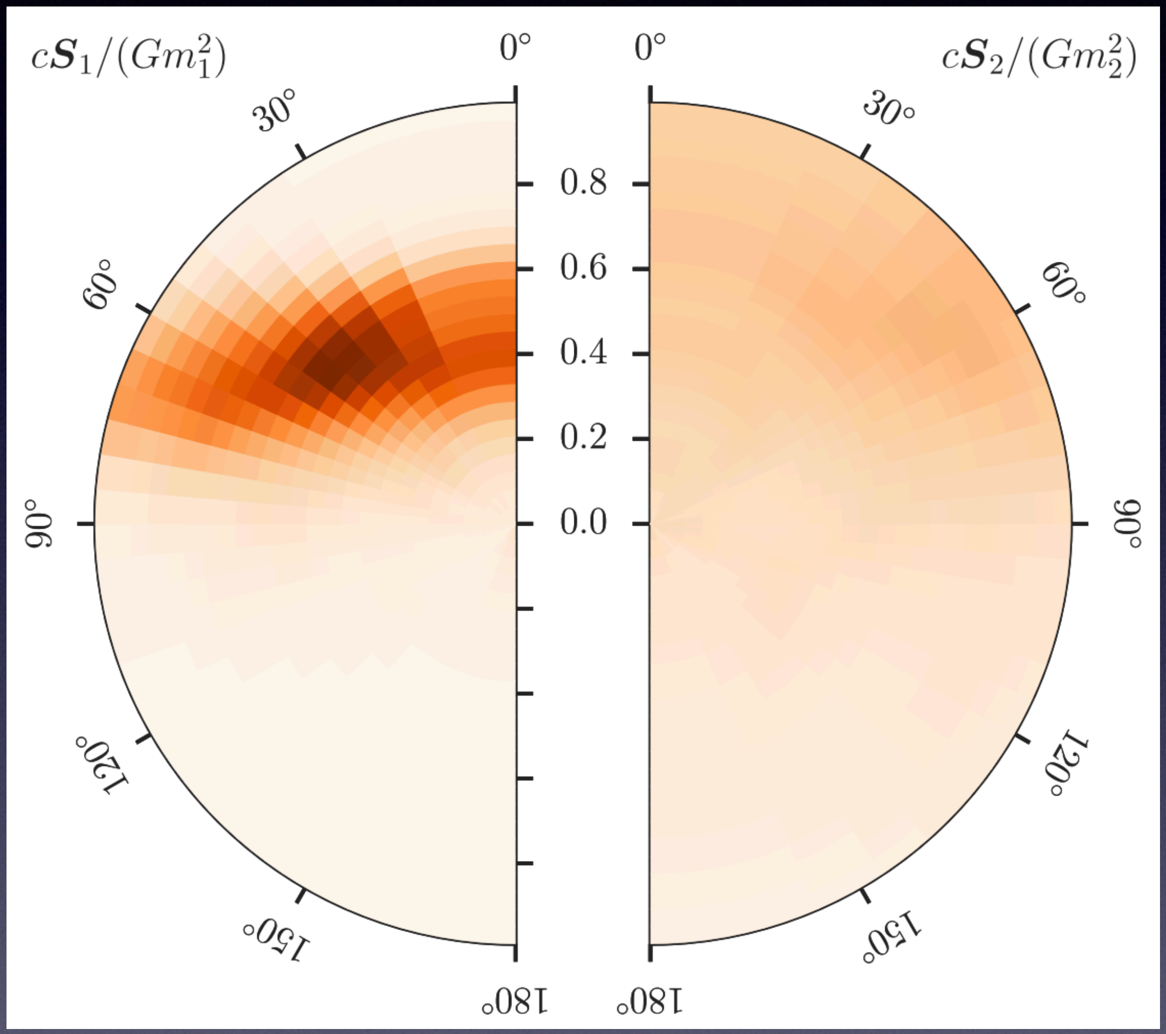

GW151226

Figures: LSC collaboration 2016, 2018

Comparison to models

Misaligned spins possible in field channel if large kicks, natural in dynamical channel

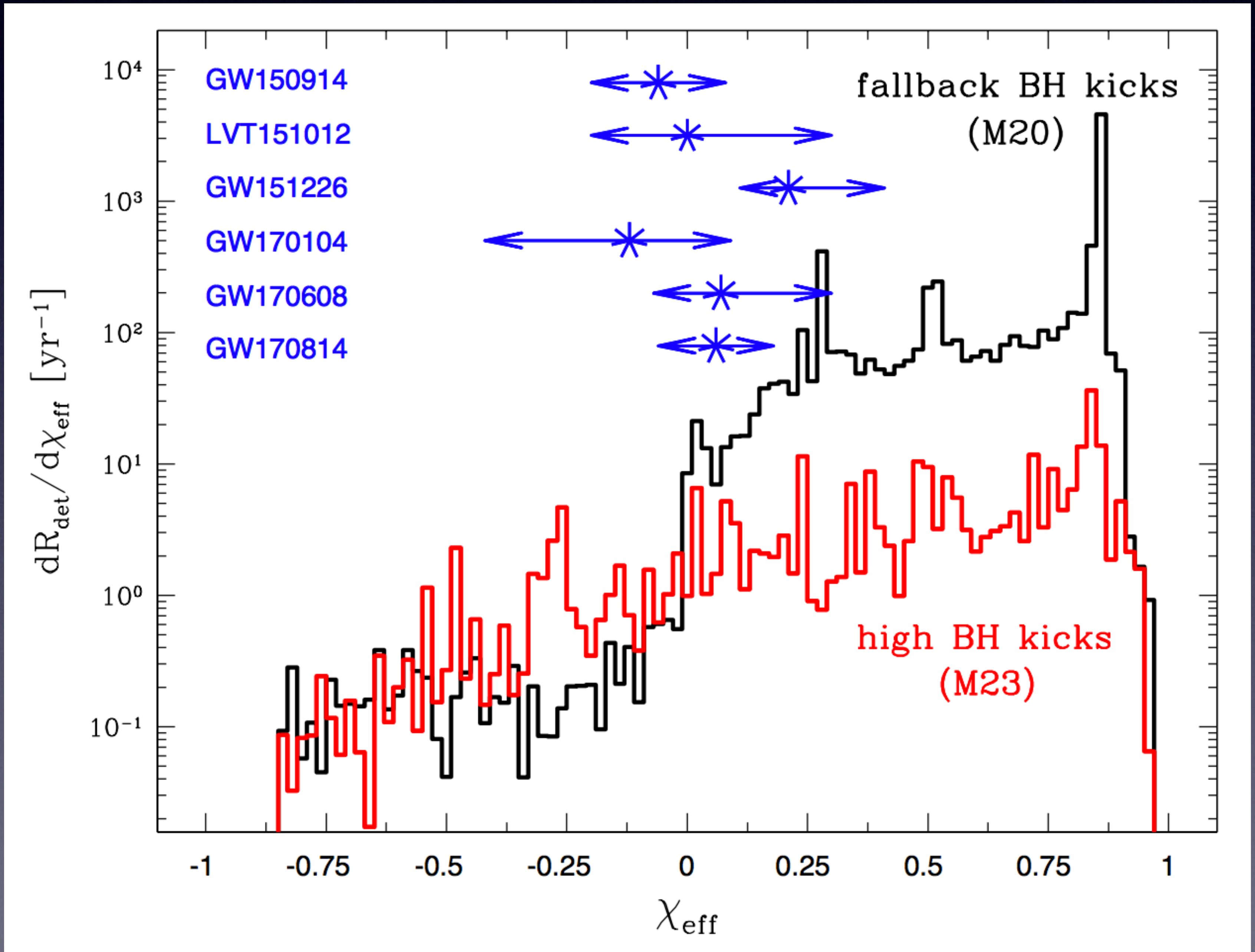

Figure from Belczynski et al 2017

GWs from binary BHs

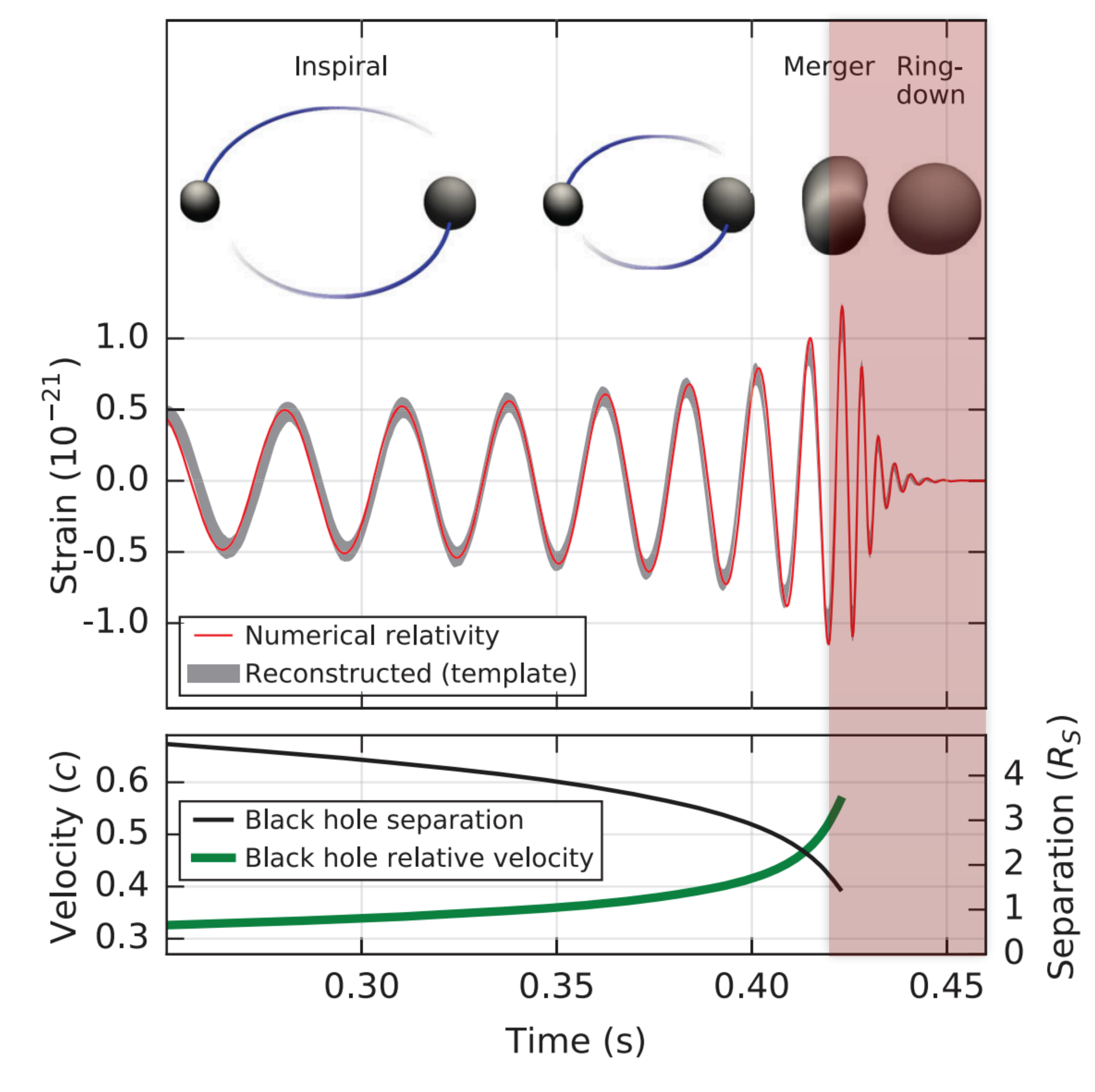

LSC collaboration 2015

Perturbations of non-spinning BHs

- Consider scalar field toy model first $g^{\mu\nu}\nabla_\mu\nabla_\nu\varphi = 0$
- On Schwarzschild, decompose in spherical harmonics

$$\varphi = \sum_{\ell,m} \frac{R_{\ell m}(r)}{r} Y_{\ell m}(\theta,\phi) e^{-i\omega t}$$

- Because of symmetry, equations “separate”:

$$\frac{\mathrm{d}^2 R}{\mathrm{d}r_*^2} + (\omega^2 - V)R = 0$$

$$r_* \equiv r + 2M \ln\left(\frac{r}{2M} - 1\right)$$

Tortoise coordinates ranging +/- ∞

$$V(r) \equiv \left(1 - \frac{2M}{r}\right)\left[\frac{l\,(l+1)}{r^2} + p\right]$$

$$p = 2M/r^3$$

BH ringdown perturbations

- Perturb Kerr/Schwarzschild BH metric ($g=g_0+h$)
- Expand in Fourier modes and (spin-weighted spheroidal) harmonics

$$\psi(t\,,r\,,\theta\,,\phi) = \frac{1}{2\pi}\int e^{-i\omega t}\sum_{l=|s|}^{\infty}\sum_{m=-l}^{l} e^{im\phi}\,{}_sS_{lm}(\theta)R_{lm}(r)d\omega$$

$$\psi = \frac{1}{2}\left(\frac{\partial^2 h_+}{\partial t^2} - i\frac{\partial^2 h_\times}{\partial t^2}\right)$$

$$\Delta\partial_r^2 R_{lm} + (s+1)(2r-2M)\partial_r R_{lm} + V R_{lm} = 0$$

- Akin to solving Schrodinger equation in 1D in quantum mechanics 101
- Discrete complex quasinormal mode frequencies
- Imaginary part of frequency shows linear stability

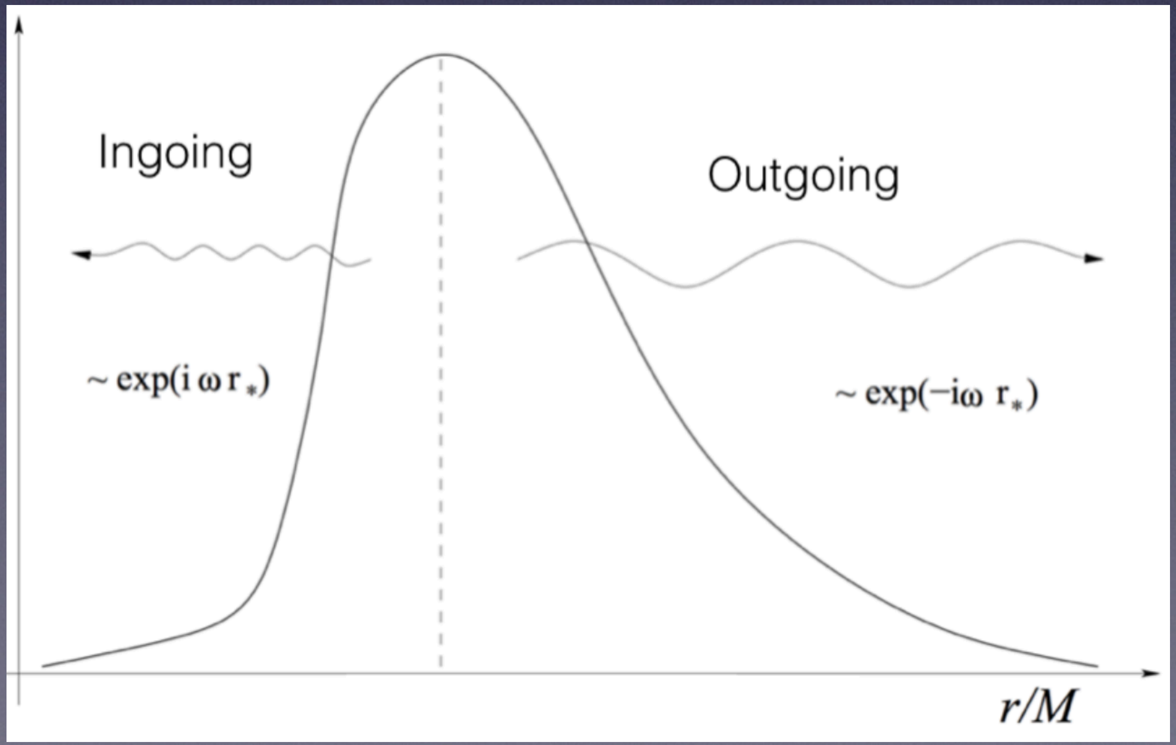

Ringdown tests of the no-hair theorem

$$\omega_{\ell m} = \omega_{\ell m}^{GR}(M,J)(1+\delta\omega_{\ell m}) \qquad \tau_{\ell m} = \tau_{\ell m}^{GR}(M,J)(1+\delta\tau_{\ell m})$$

- Difficult with advanced detectors because little SNR in ringdown: need LISA/3G

- Can perform consistency tests between merger/ringdown

- Connection to circular photon orbit frequency ω and Lyapunov coefficient λ (i.e. curvature of geodesics effective potential) in geometric optics limit!

$$\omega_{ln}^{m=l} \approx l\omega_{+} - i\lambda_{+}(n+1/2)$$

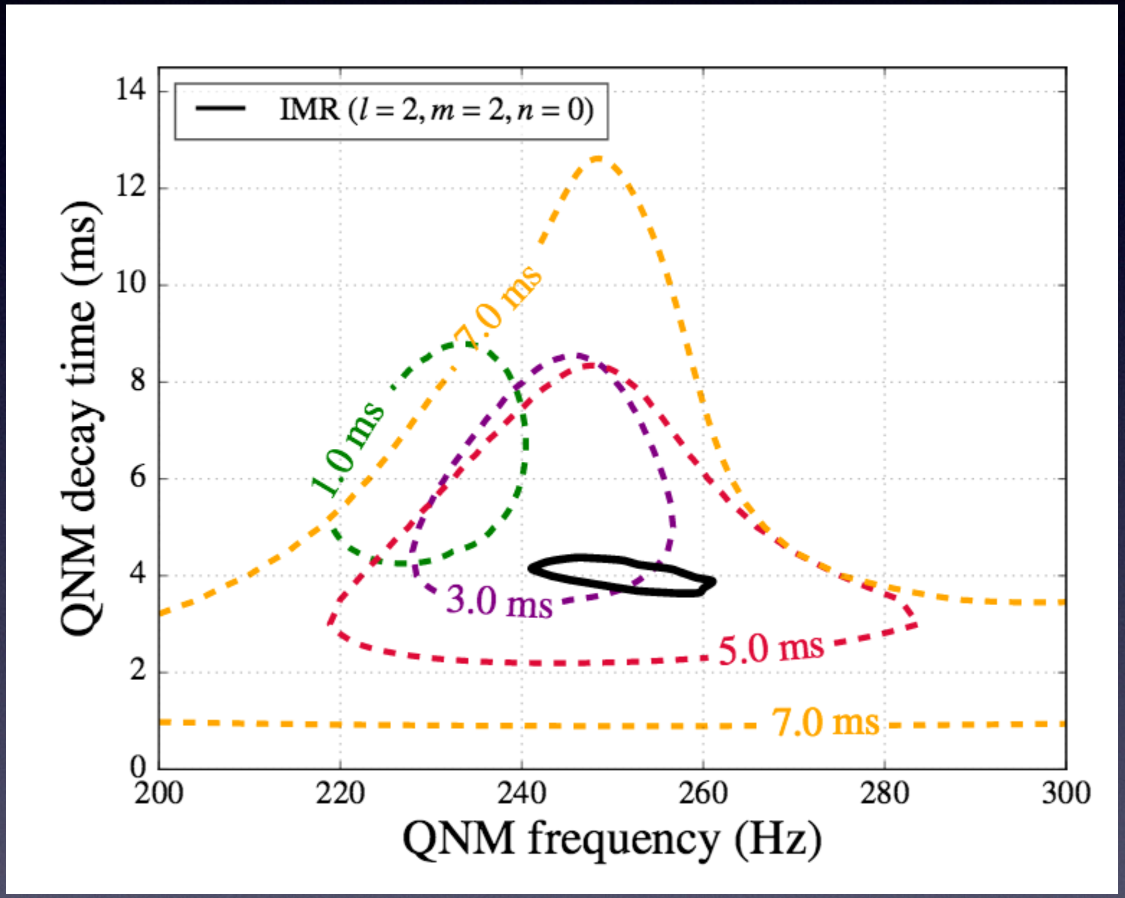

From the LSC paper on tests of GR

Null geodesics in Schwarzschild/Kerr

- Dynamics only depends on b=L/E (and spin)
- In Schwarzschild (Kerr qualitatively the same but for frame dragging):

$$\frac{1}{E^2}\left(\frac{dr}{d\lambda}\right)^2 = -V = 1 - \frac{b^2}{r^2}\left(1 - \frac{2GM}{r}\right)$$

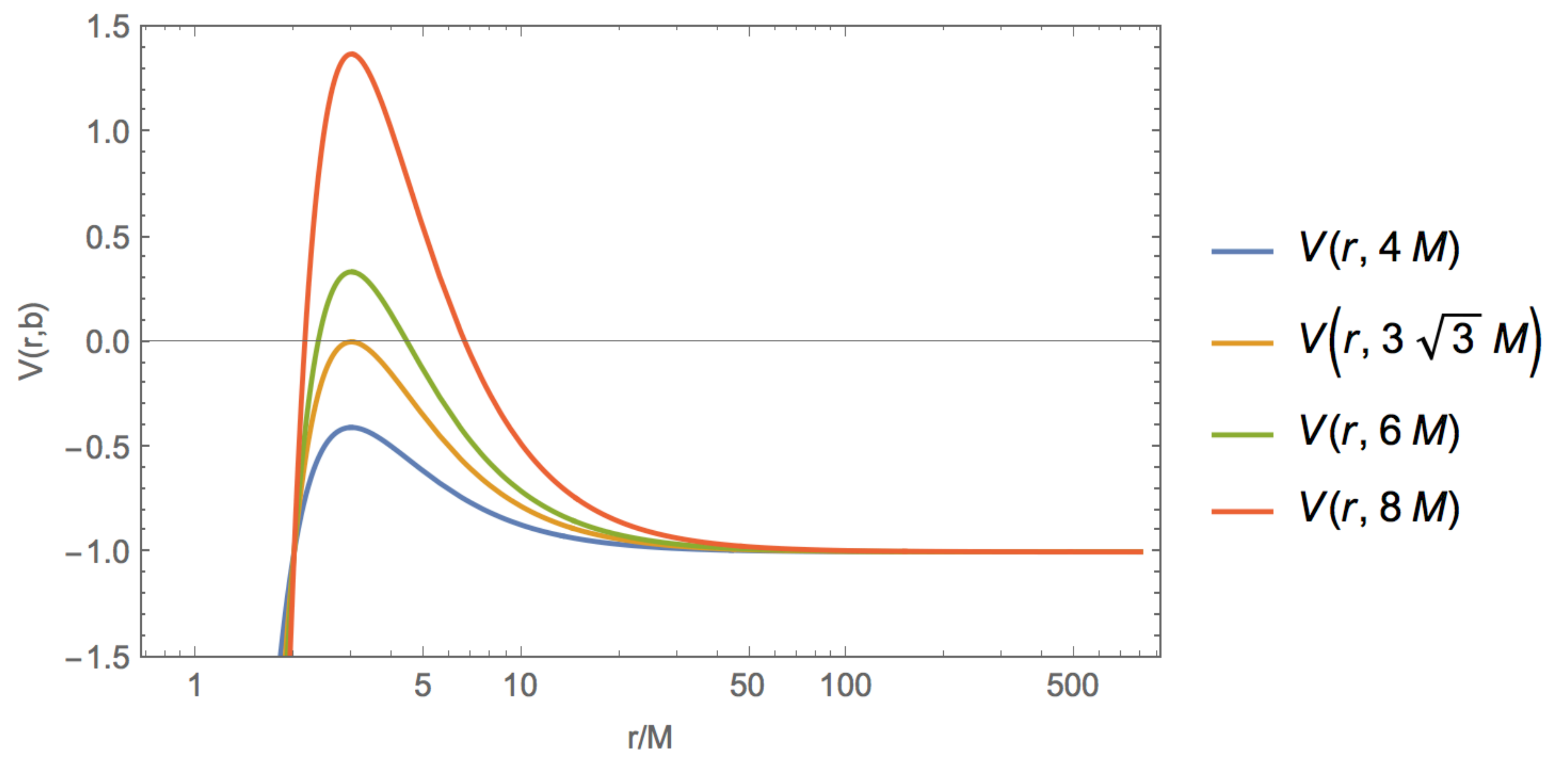

- (Unstable) circular photon orbit ("light ring") at r=3M

- Peak of "potential barrier" at r=3M (same as for QNM potential, because of geometric optics limit)

BH shadows

Event Horizon Telescope
will image SgrA* and M87
via VLBI radio (mm wavelength)
observations

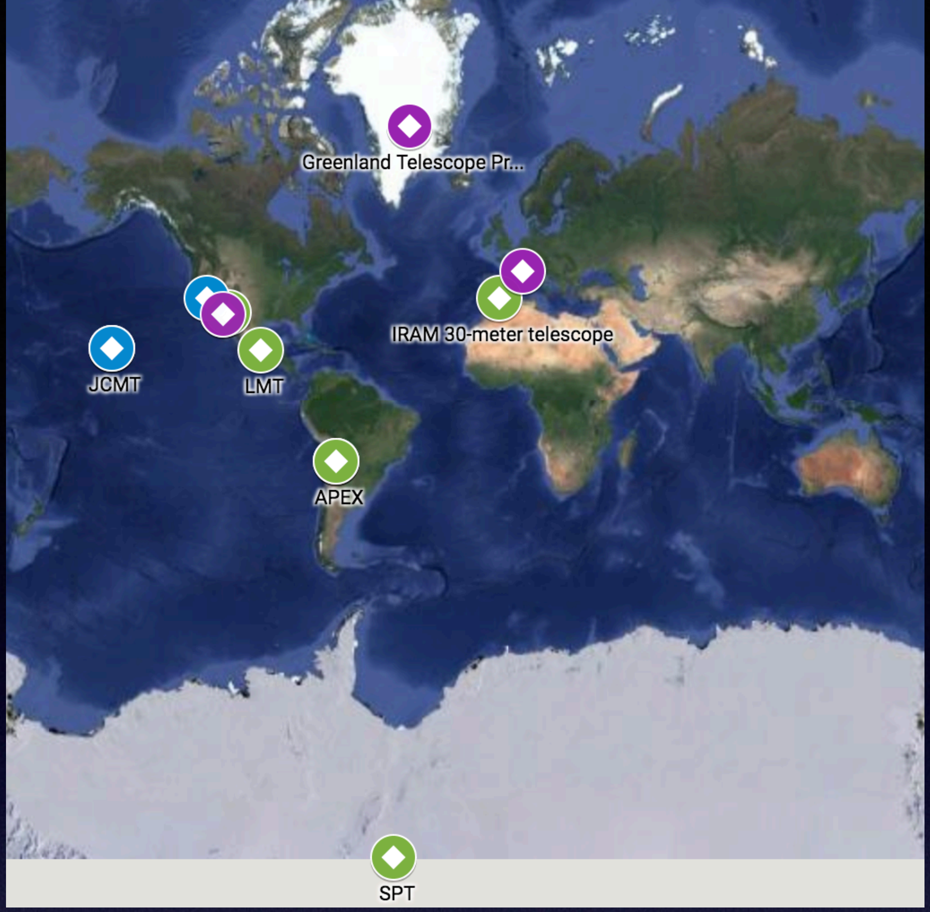

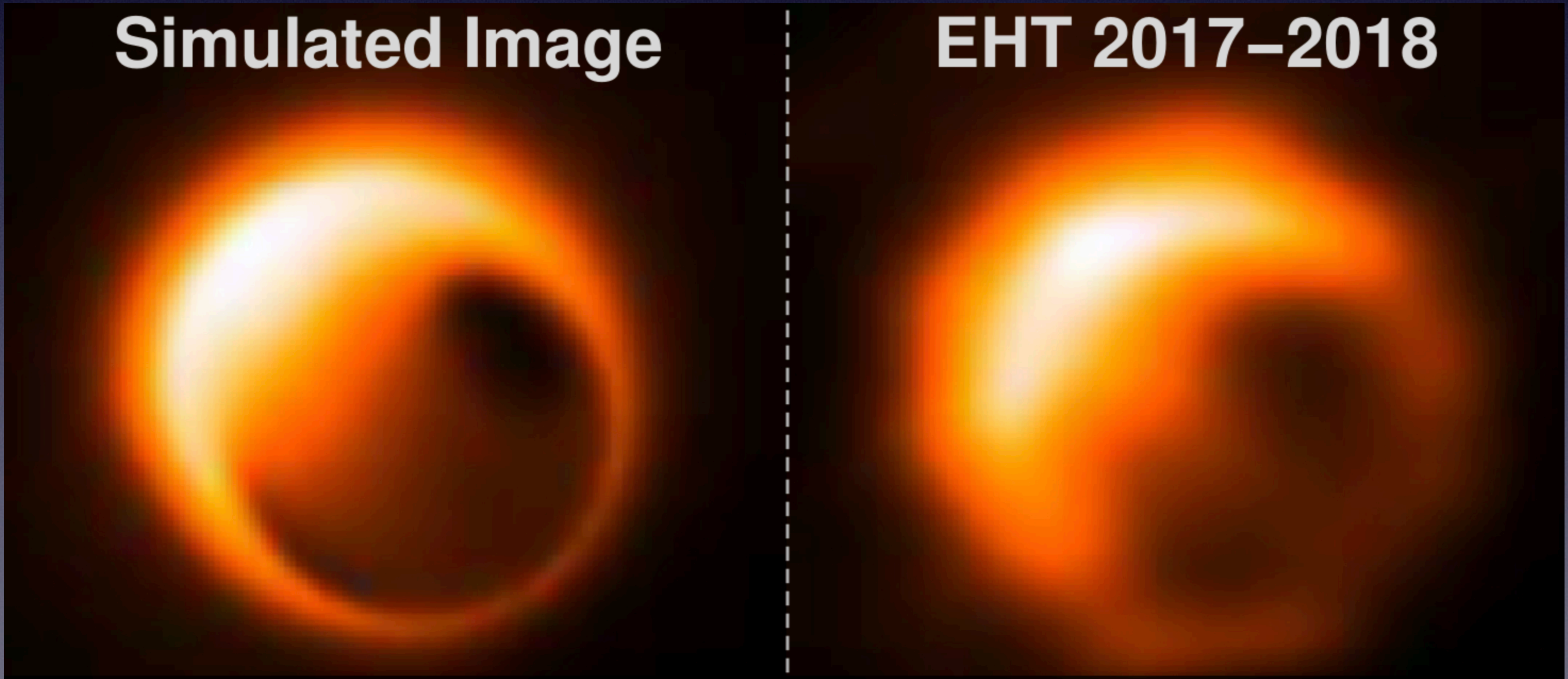

Imaging a Black Hole. At left is a model image for Sgr A* using a semi-analytic accretion flow (Broderick et al. 2011). Light is gravitationally lensed by the black hole to form a distinctive "ring" encircling the black hole's "shadow" (Falcke et al. 2000). The ring diameter is ~5 Schwarzschild radii . The image is bright on the approaching side of the accretion disk and faint on the receding side because of Doppler effects. At right, a sample image shows expected EHT performance in 2017-2018 (Fish, Johnson, et al. 2014).

LIGO's are not the biggest BHs in the Universe!

A monster of 4.5 million solar masses in the centre of our Galaxy!

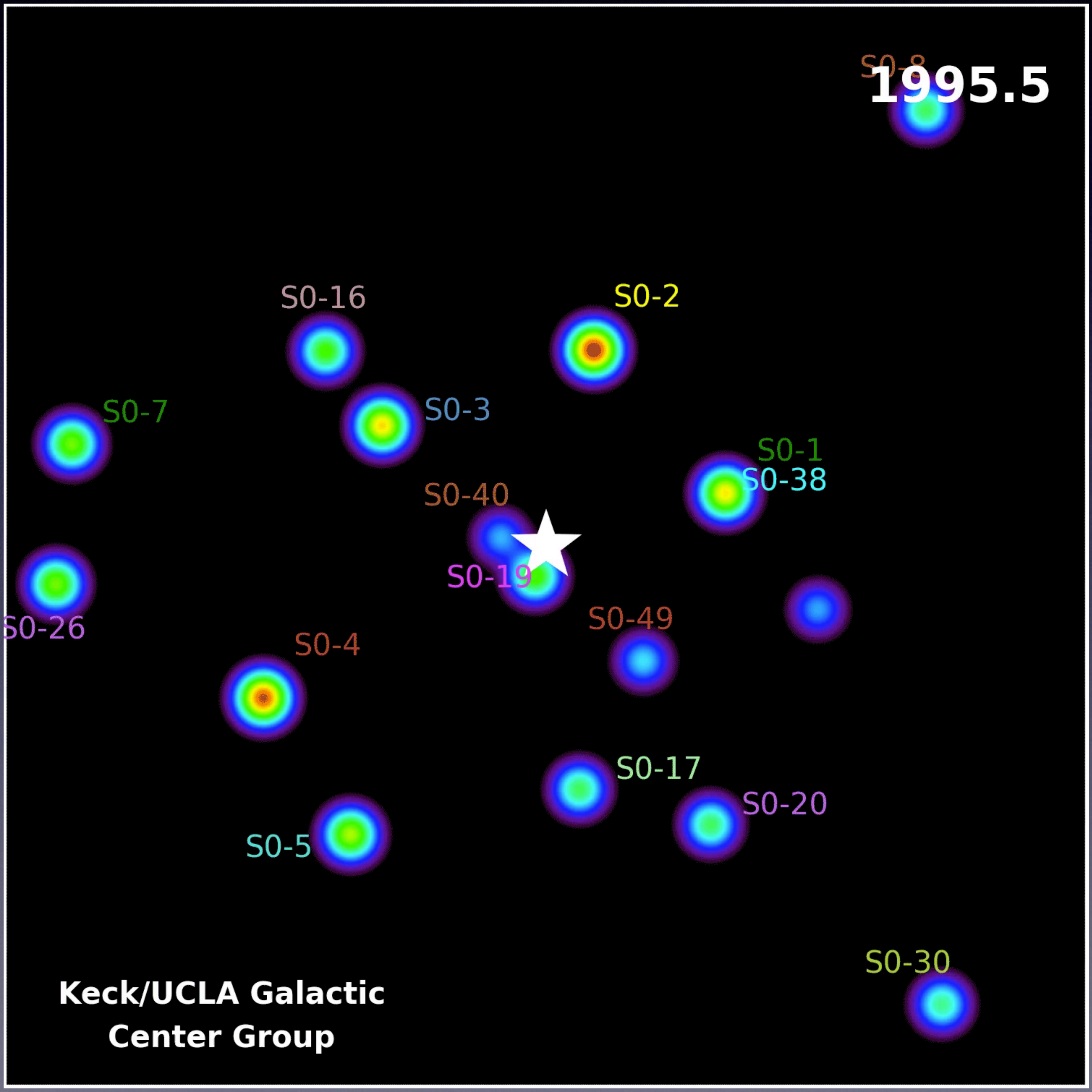

Galaxies merge…

… so massive BHs must merge too!

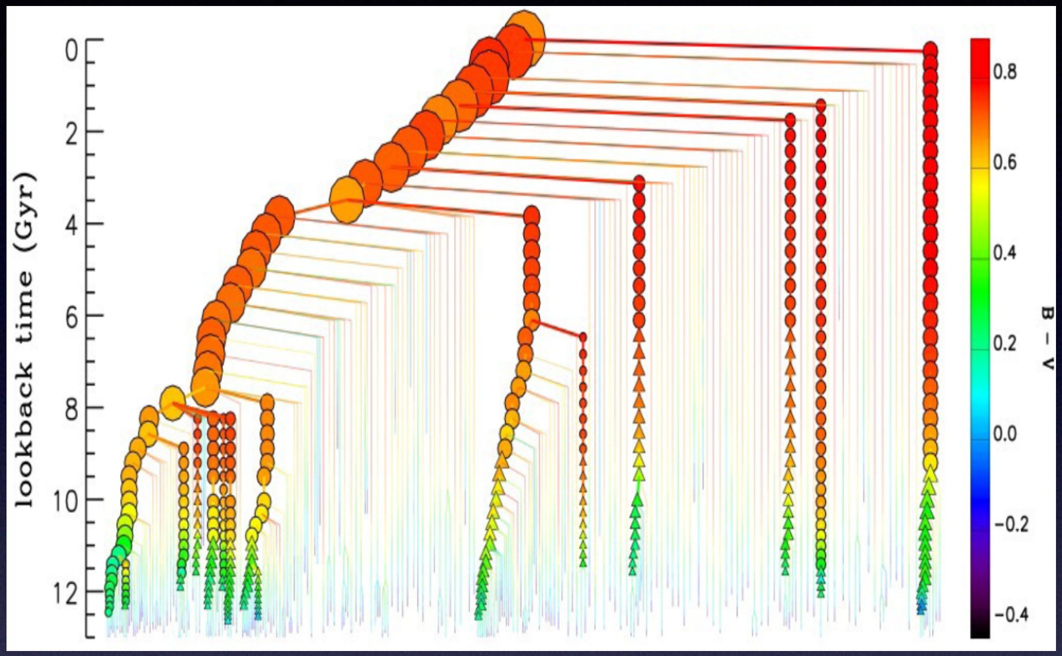

Figure from De Lucia & Blaizot 2007

+

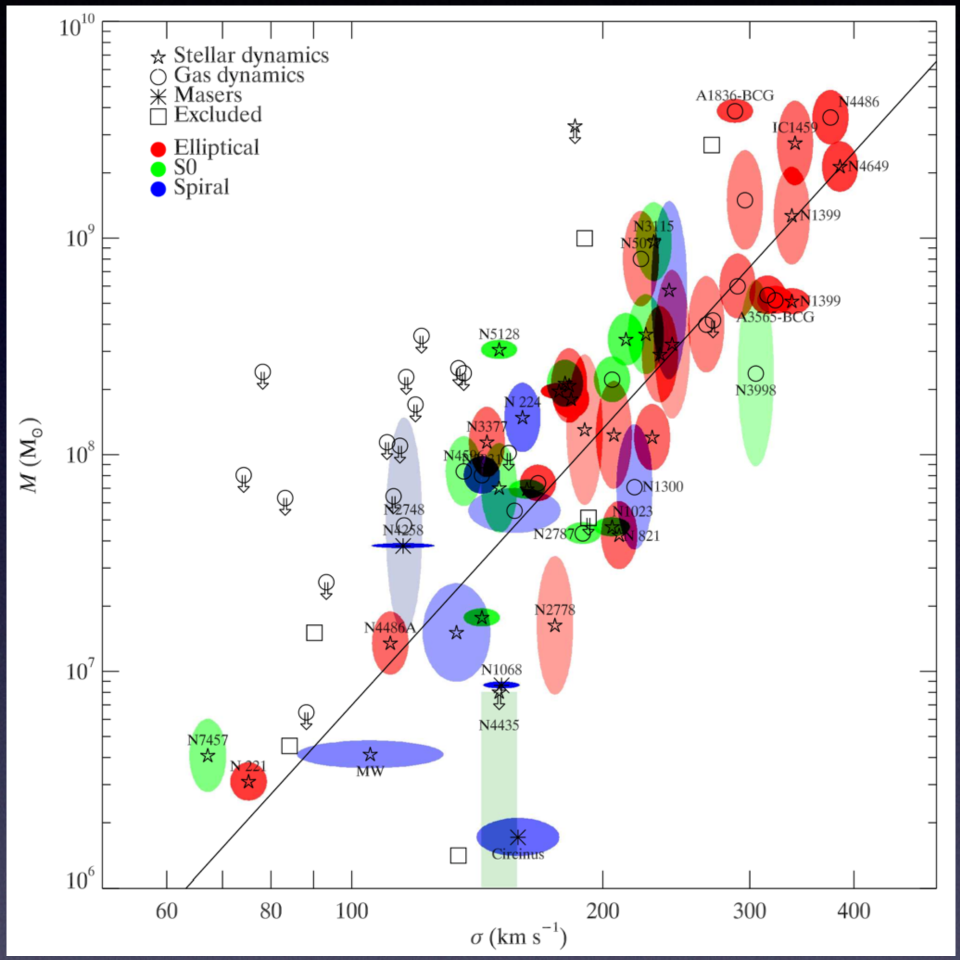

Ferrarese & Merritt 2000
Gebhardt et al. 2000,
Gültekin et al (2009)

=

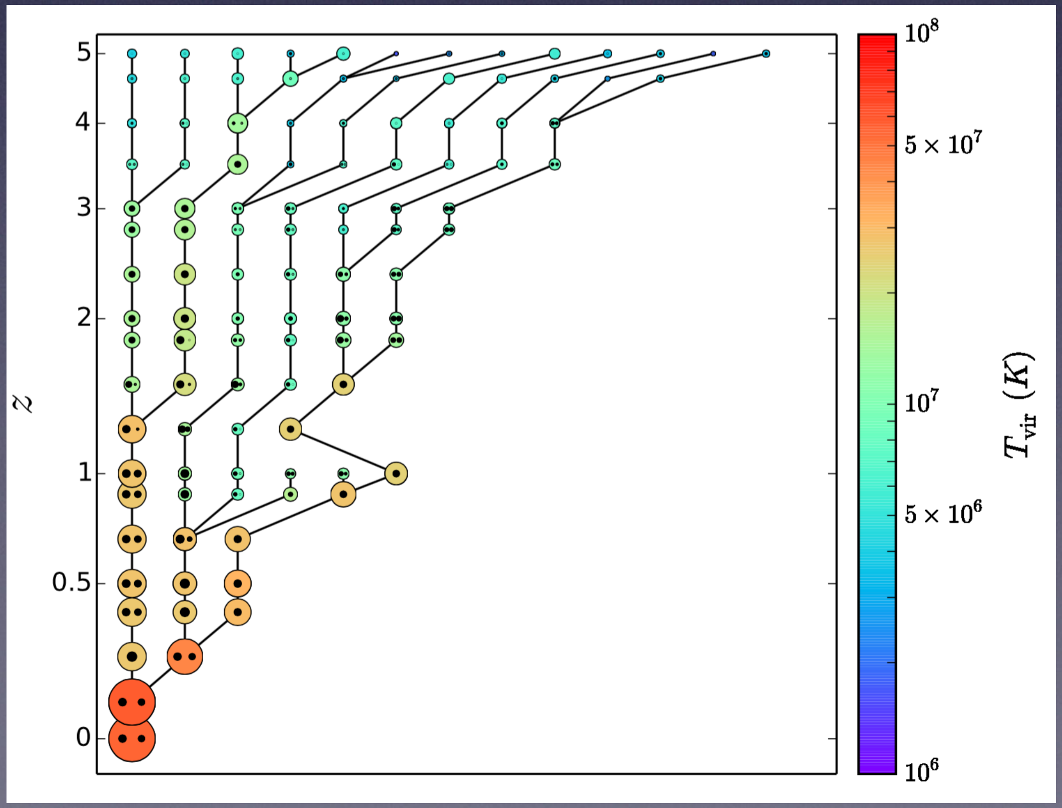

EB 2012
Figure credits: Lucy Ward

What links large and small scale?

- Small to large: BH jets or disk winds transfer kinetic energy to the galaxy and keep it “hot”, quenching star formation (”AGN feedback”). Needed to reconcile ΛCDM bottom-up structure formation with observed “downsizing” of cosmic galaxies

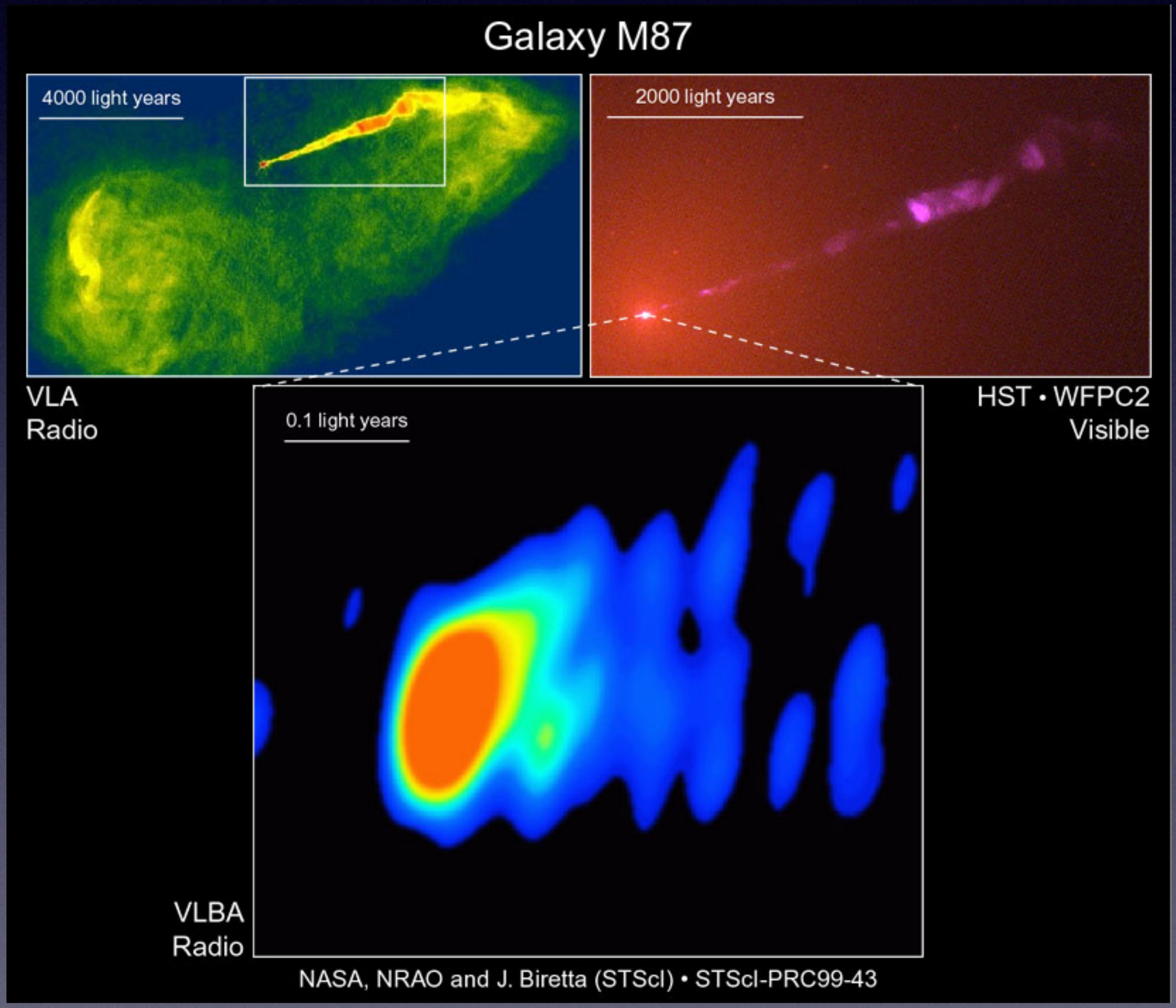

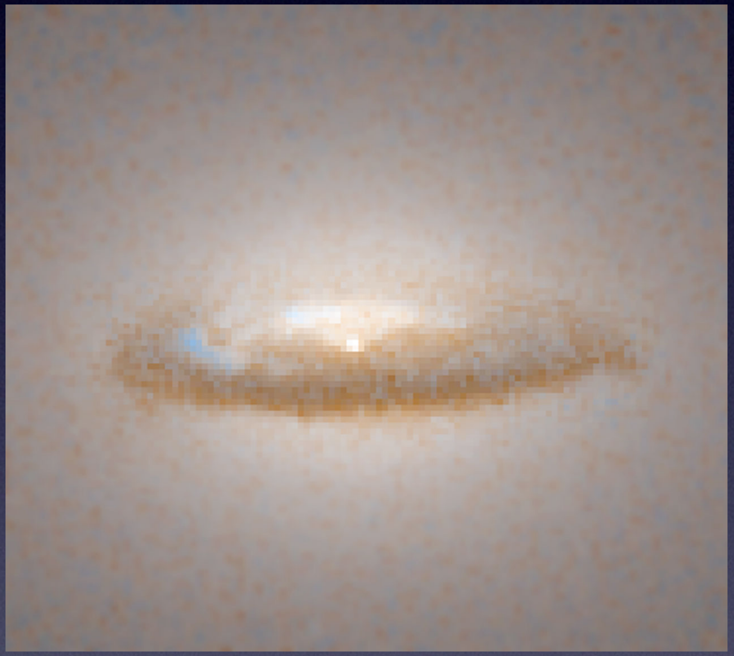

Disk of dust and gas around the massive BH in NGC 7052

- Large to small: galaxies provide fuel to BHs to grow (”accretion”)

GWs from massive BHs

$$f_{\rm GW} = \frac{6 \times 10^4}{\tilde{m}\tilde{R}^{3/2}}\,\text{Hz} \qquad \tilde{R} = R/(Gm/c^2)$$
$$\tilde{m} = m/M_\odot$$

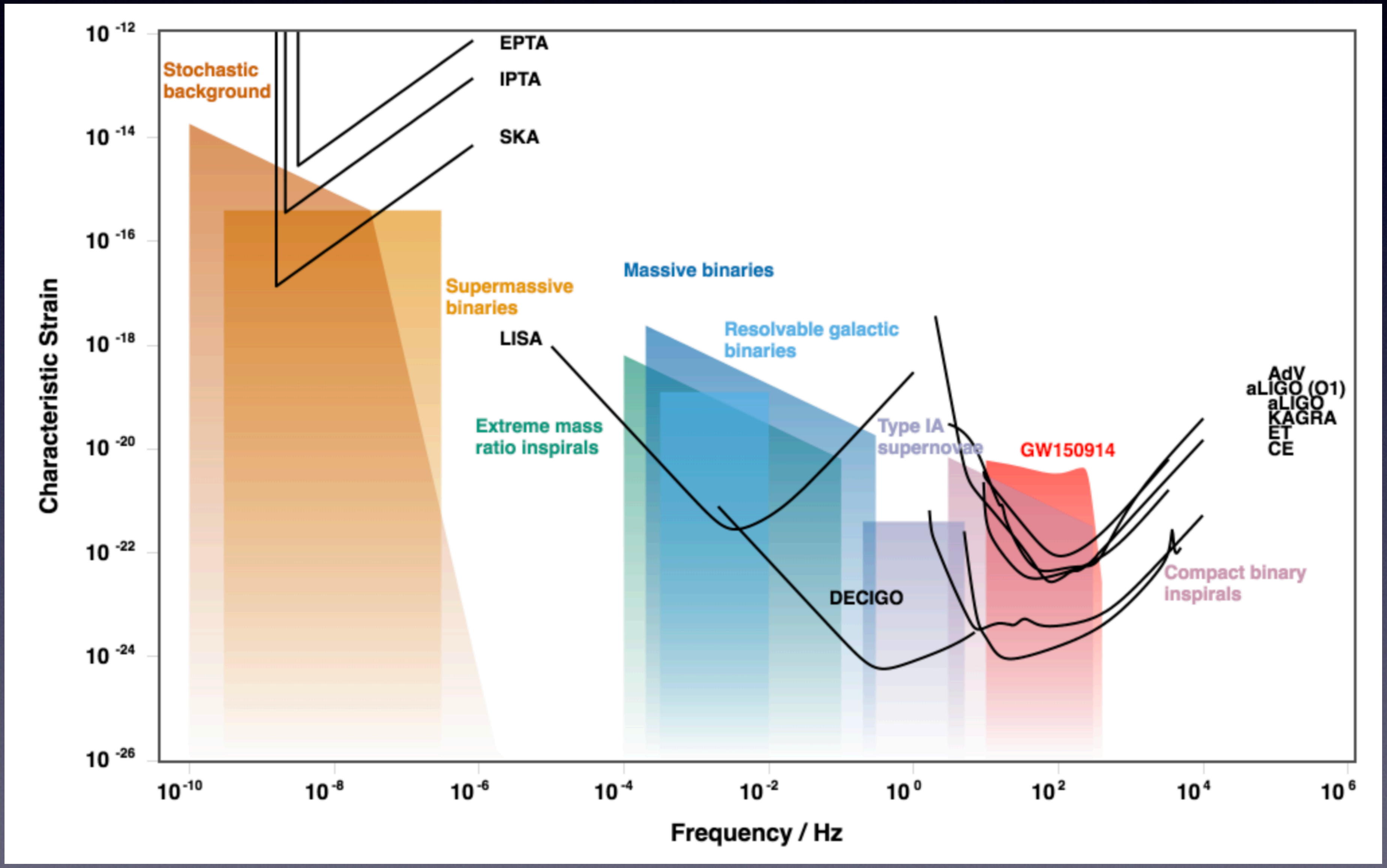

Figure generated by http://gwplotter.com

Problem: terrestrial detectors blind at f ≲ 1-10 Hz (seismic noise)

The space race!

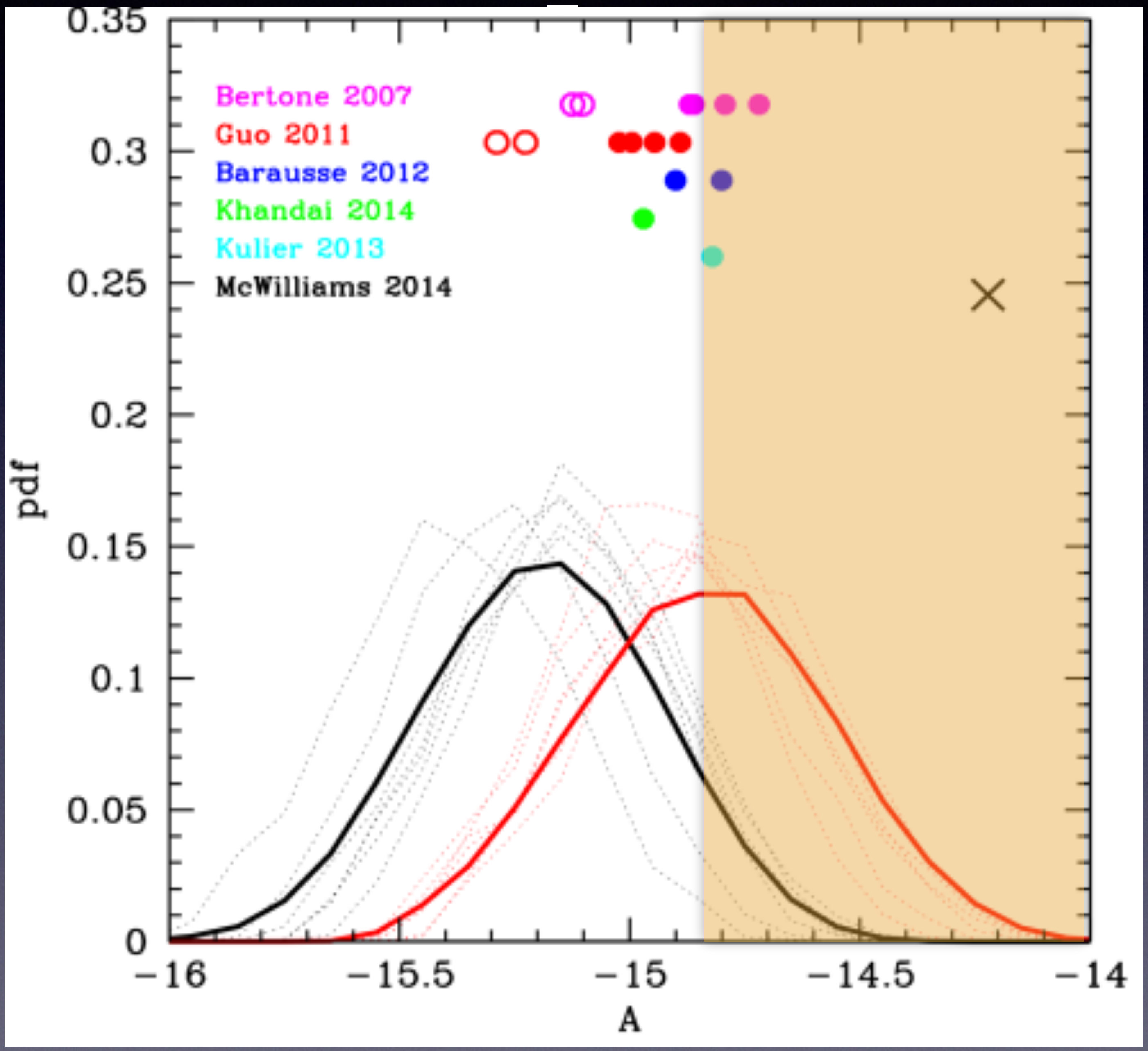

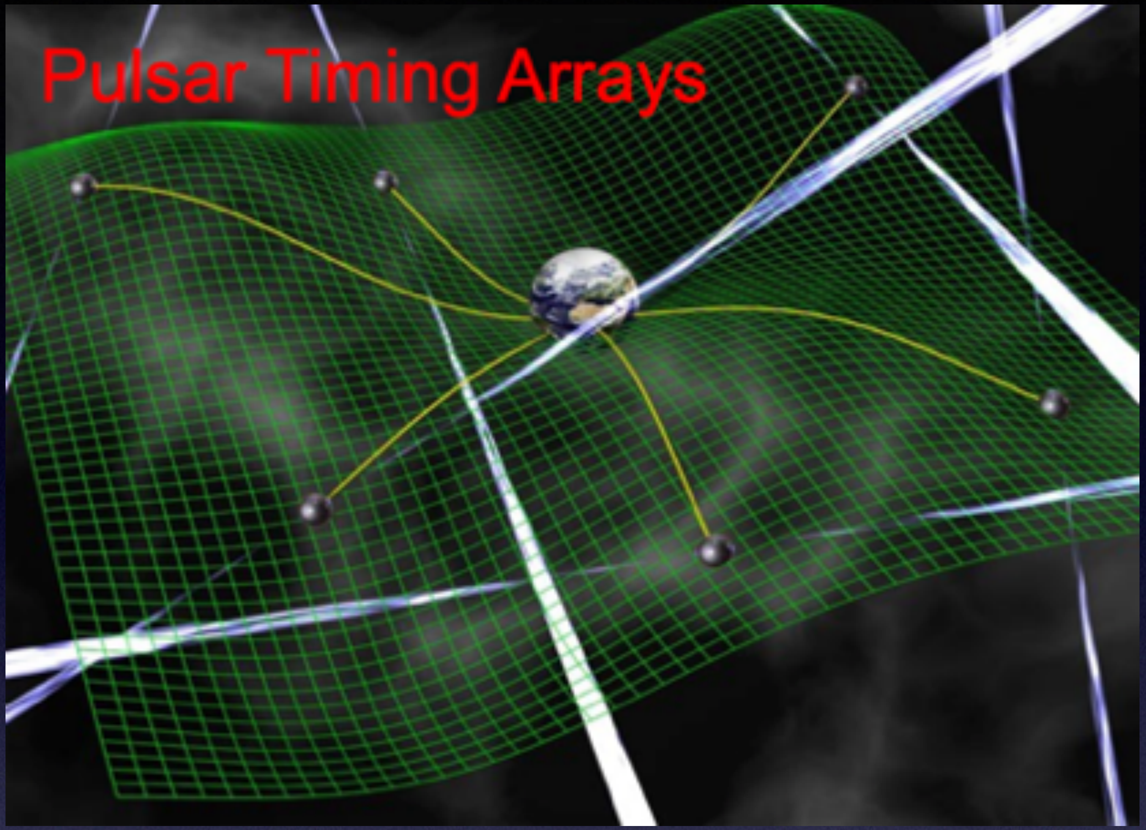

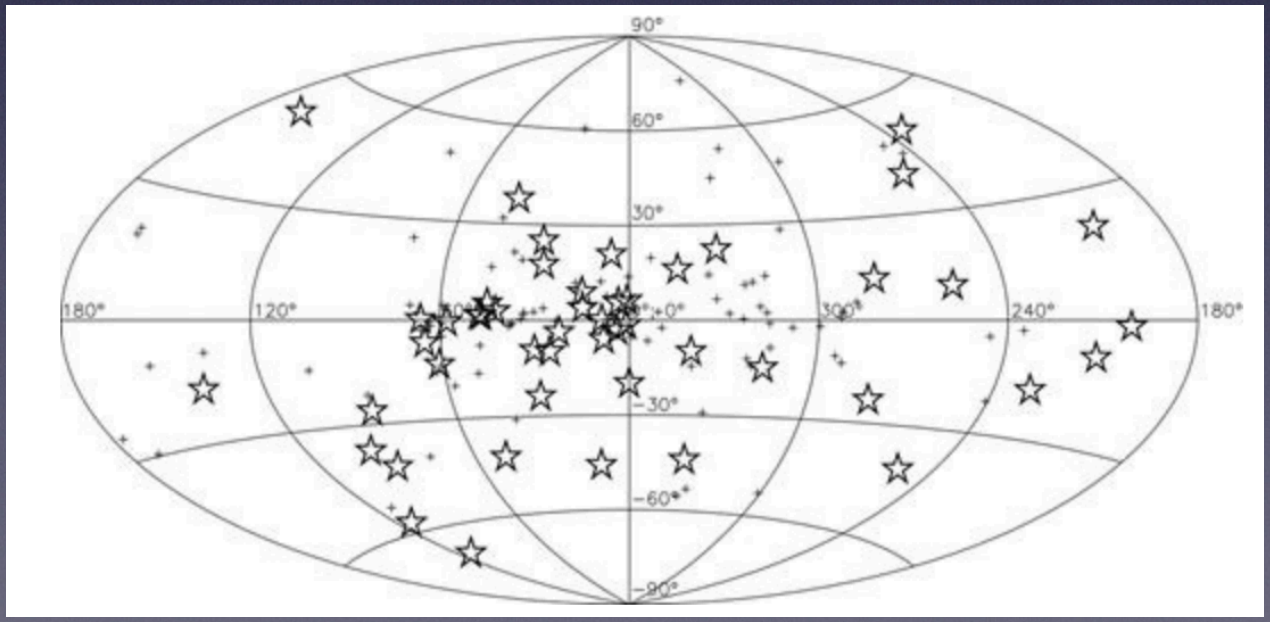

Background characteristic strain at f=1/yr is A<1.45 x 10^{-15} (Nanograv 2018)

Laser Interferometer Space Antenna (LISA)

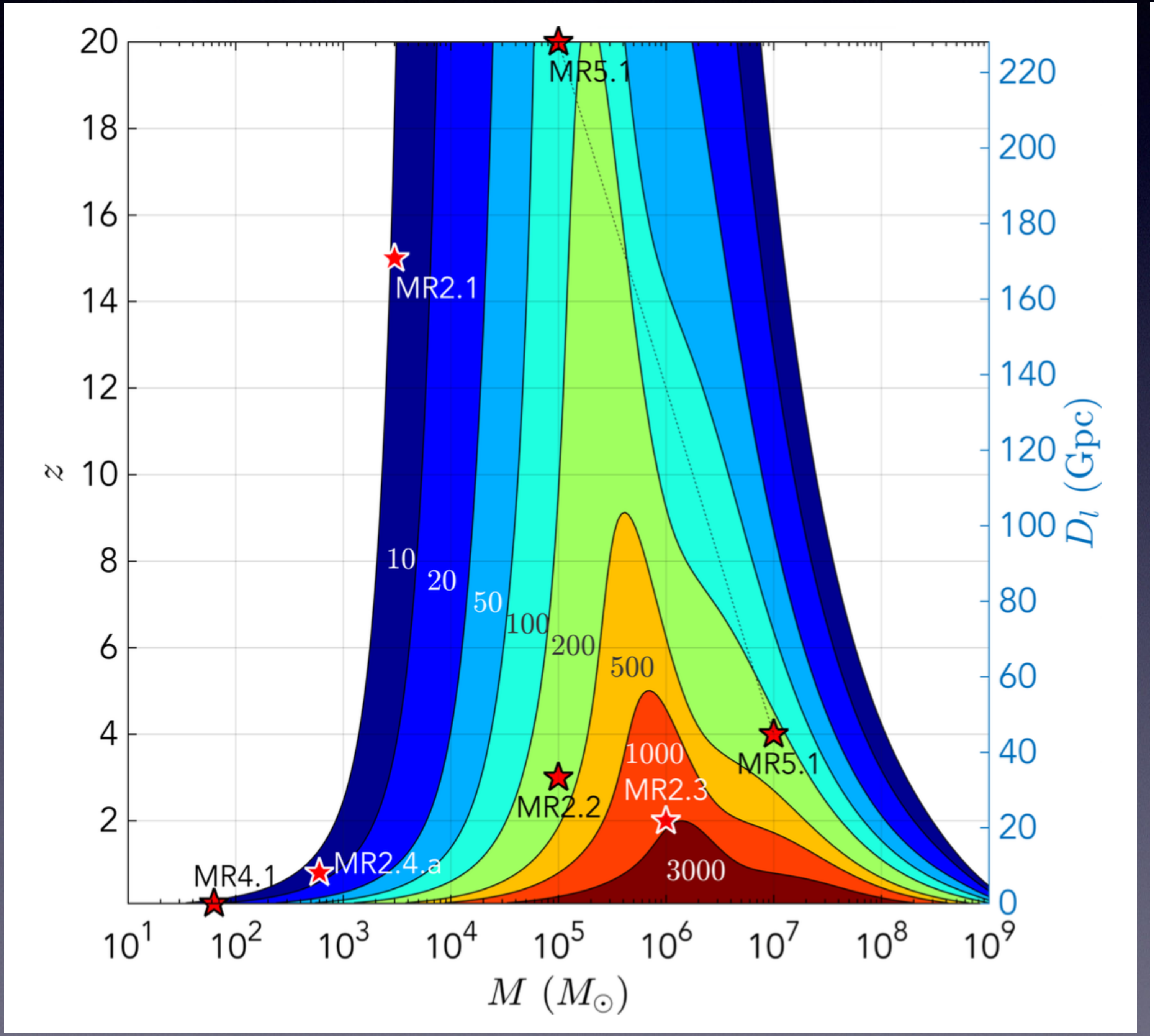

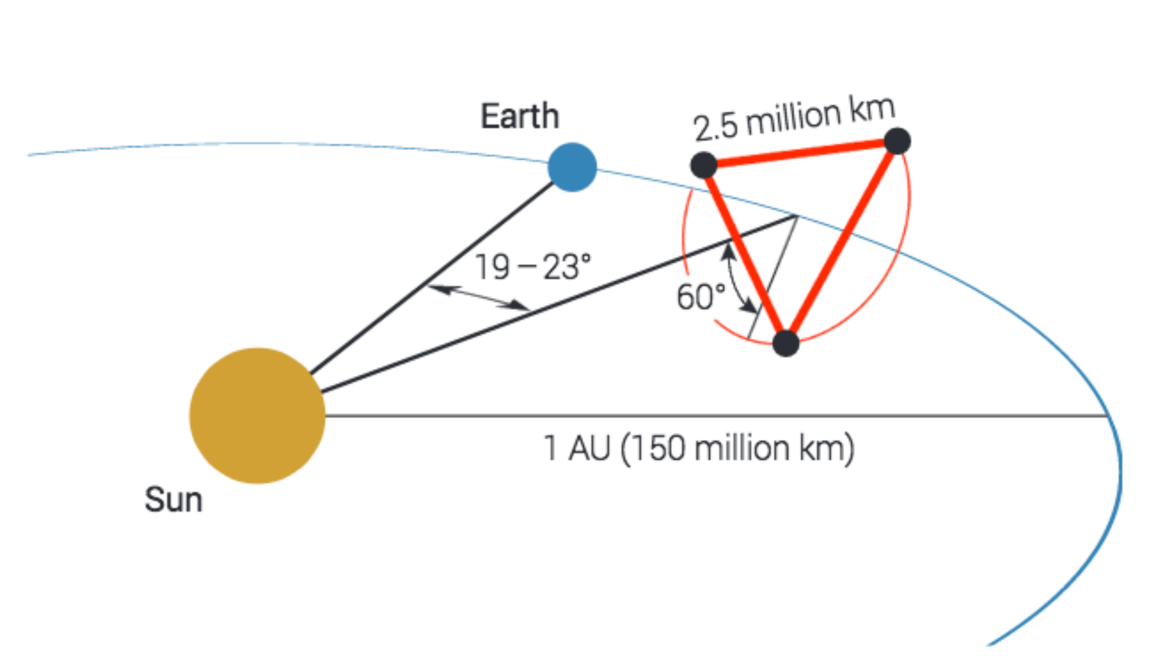

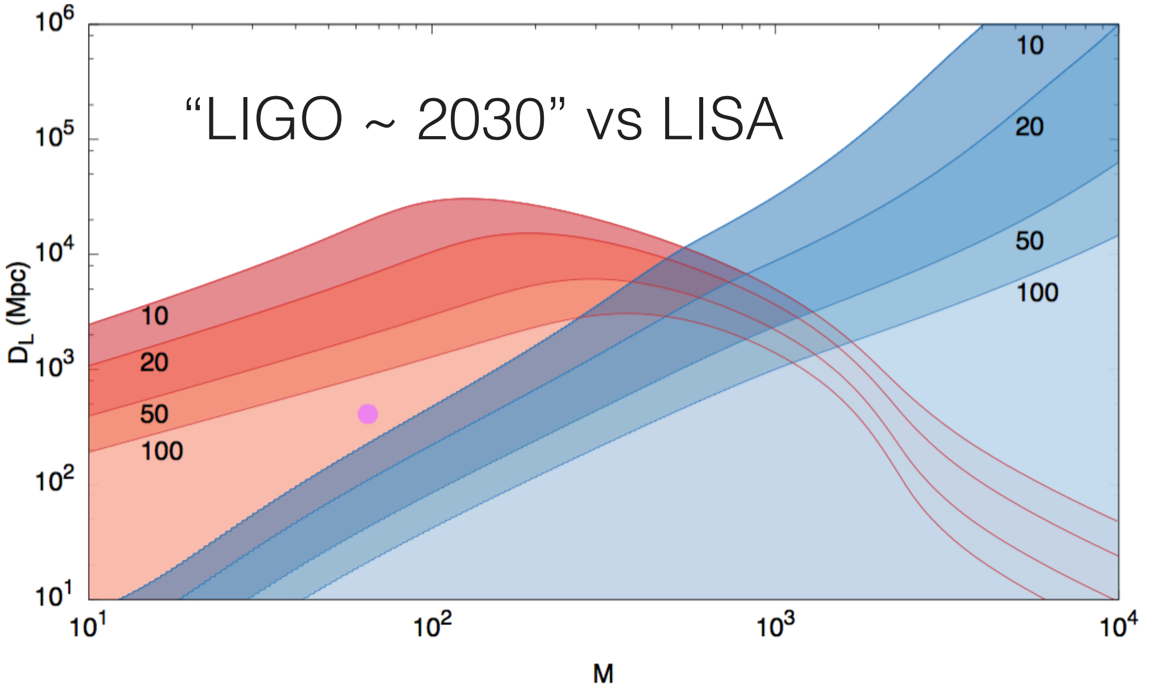

Multi-band gravitational-wave astronomy

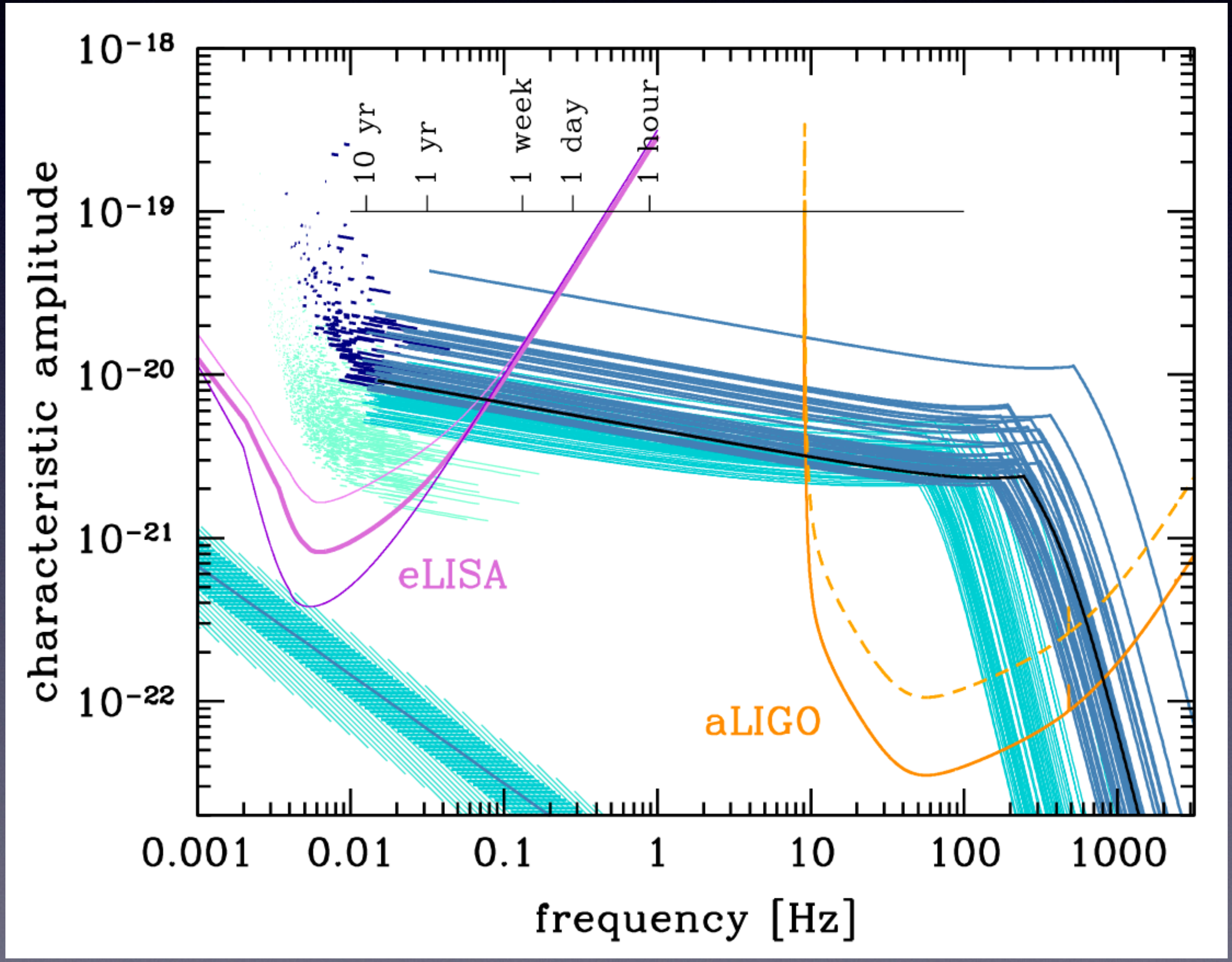

Sesana 2016

LISA status and timeline

- LISA Pathfinder mission a success (surprisingly stable)
- LISA is now a mission (June 2017)
- Phase 0 ended; currently (2018-19) in Phase A, then ~ 10 yrs of industrial production, with launch ~ 2030-34
- Phase 0/A: finalization of mission design (options analyzed by ESA's Gravitational Wave Advisory Team in collaboration with industry & LISA Consortium) + consortium re-organization

The LISA Data Challenge and the enchilada problem

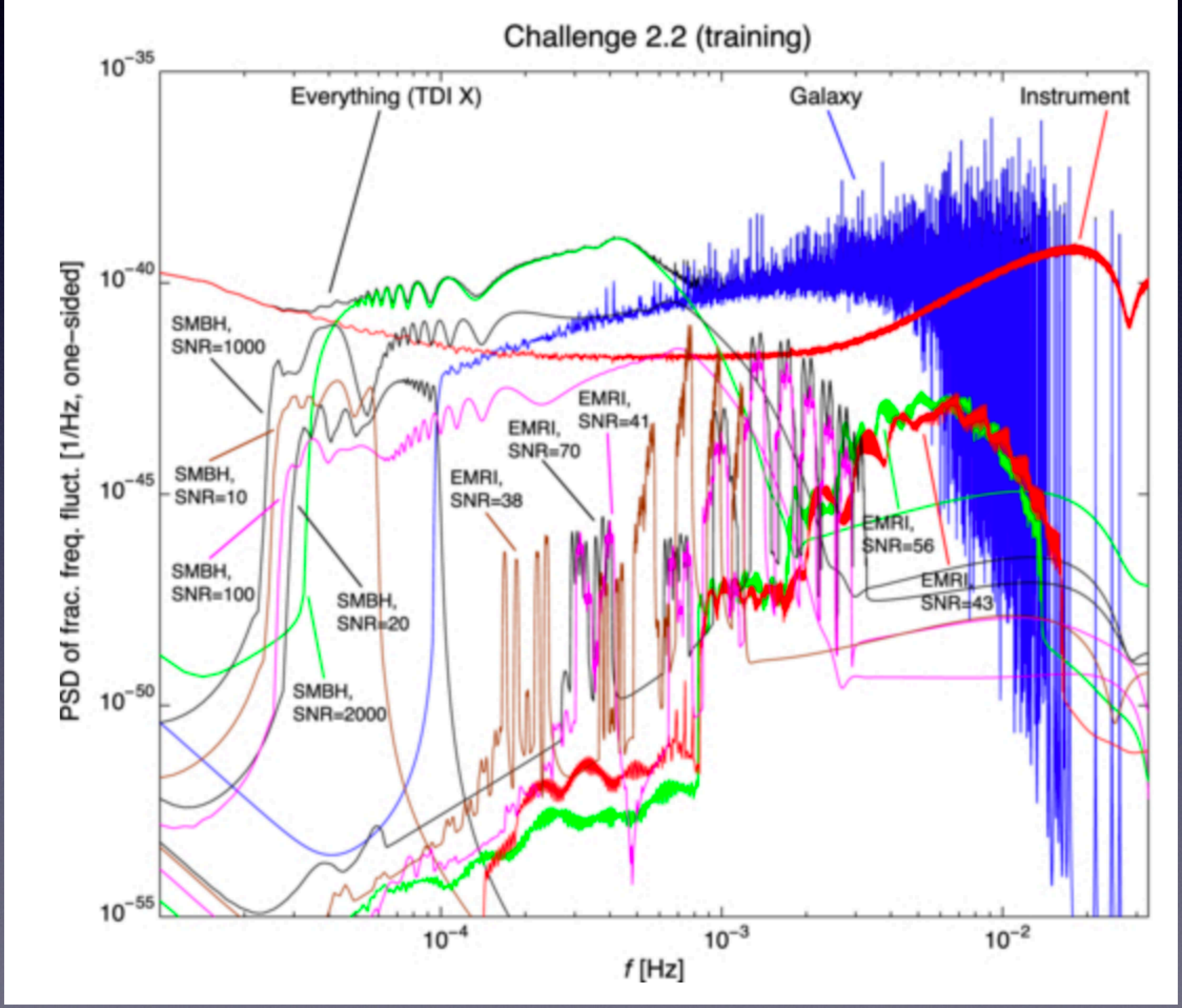

https://signup.lisamission.org/